AN INVESTIGATION OF MALTOL COMPLEXES OF ALUMINIUM, INDIUM AND GADOLINIUM

A thesis submitted to the

UNIVERSITY OF CAPE TOWN

in fulfillment of the requirements for the degree of

MASTER OF SCIENCE

by

Charlene B. Steyn

BSc(Hons) (Cape Town)

Department of Chemistry
University of Cape Town
Rondebosch
7700
South Africa

October 1989

2.3 EXPERIMENTAL

2.3.1 Reagents

All solutions were prepared in glass distilled, deionised water, which had been boiled to remove dissolved CO_2. The ionic strength was maintained at 0.15M using NaCl.

The maltol (Sigma Chemical Co.) was used without further purification. Elemental analysis and potentiometric titration showed the ligand to have a purity >99%.

NaOH was supplied by BDH Chemicals Ltd. The NaOH solutions were standardised by titration against potassium hydrogen phthalate. The potassium hydrogen phthalate was recrystallised before use according to the procedure described by Vogel [2].

Gadolinium and indium nitrates (Aldrich Chemical Co.) were of analytical grade. Stock solutions of these were prepared and standardized by EDTA titration. The aluminium chloride (SARCHEM Ltd) was of analytical grade. A stock solution was prepared and standardised by back-titration of EDTA with $ZnSO_4$ solution.

All the metal stock solutions were analysed for hydrogen ion concentration using Gran's method [3] of potentiometric titration

2.3.2. Potentiometric Titration

All titrations were carried out at 25 ±0.1 °C in a Metrohm titrating vessel using carbonate free sodium hydroxide.

The titrations were carried out in a cell of the type indicated in the diagram.

Silver-silver chloride reference electrode	0.15M NaCl	‖	Experimental solution in titration vessel	glass electrode

The titrations were carried out under an oxygen free, nitrogen atmosphere. The nitrogen was purified by successive washing in

(i) 15% pyrocatechol in 30% potassium hydroxide solution to remove O_2 and CO_2.

(ii) 50% potassium hydroxide solution to remove CO_2.

(iii) 0.15M NaCl solution.

The general procedure involved the potentiometric titration of several solutions of different metal: ligand ratios and concentrations with standard NaOH. The ligand protonation constant was determined from solutions containing no metal ions.

Both the metal ion solution and the ligand solution were added to the titration vessel using Metrohm burettes which could be read with an accuracy of ±0.005ml.

The reaction was followed using a Metrohm glass electrode and a silver-silver chloride reference electrode, the latter having a renewable liquid junction of 0.15M chloride concentration.

The emf readings were taken on a Radiometer PHM 84 digital pH-meter which was interfaced with a computer (South West Tech.) programmed only to collect data once on emf drift $<0.1\ mVmin^{-1}$ was established.

The electrodes were calibrated using standardised HCl and the electrode intercept, E^o, in equation 2.1 refined using the mathematical optimizations of ESTA [4] (See computations).

$$E = E^o + F_N \log[H^+] \qquad \ldots \quad (2.1)$$

The F_N term replaces 2.303/RT in the normal Nernstian equation and takes into account any deviation from Nernstian behaviour.

2.3.3 Computation

Various computational methods exist for the calculation of stability constants [6].

The program, ESTA, was used in the current study. ESTA is a suite of computer programs and subprograms described by Murray and May [4].

By using ESTA (Equilibrium Simulation for Titration Analysis) a single value for almost any of the parameters which characterise a titration can be calculated by setting up and solving the relevant mass balance equations. The facilities also exist whereby a "best" value for a

particular parameter can be determined, based on a least square procedure over a whole system of titrations.

The optimization facilities of ESTA enable the refinement of combinations of the following parameters: vessel and burette concentrations, formation constants, electrode intercept and slope and initial vessel volume.

The simultaneous optimization of N_p parameters, P_k, is performed by the Gauss Newton method of minimizing an objective function, U, defined as.

$$U = (N-n_p)^{-1}\Sigma n_e^{-1}\Sigma W_{ni}(Y_{ni}^{0} - Y_{ni}^{c})^2$$

Where N = total number of experimental titration points

n_e = total number of electrodes

W_{ni} = weight of the i^{th} residual at the n^{th} point

Y_{ni} = T_{ni} = total concentration of component i

or E_{ni} = emf of electrode i at n^{th} titration point

(o = observed, c = calculate).

The graphic facilities allow one to obtain various plots of $\bar{Z}_H$ versus pH or $\bar{Z}_M$ vs pA. These formation curves are called $\bar{Z}$-plots and gives a pictorial representation of the equilibria occurring. If only mononuclear binary complexes are formed in solution, $\bar{Z}$ is independent of the total component concentration and all the formation curves should overlap.

In order to test the validity of a proposed model of the species present in solution and the refined β's, a set of titration data can be generated using the refined β's and then plotting a theoretical $\bar{Z}$PLOT. This "pseudoplotting" is easily done by ESTA. If the theoretical and experimental formation curves are superimposable, the model is assumed to be valid.

A measure of the agreement between experimental and theoretical data is given in the form of the crystallographic Hamilton *R*-factor [5].

$$R = (U/\Sigma n_e^{-1}\Sigma w_{ni}(Y_{ni}^{0})^2)^{\frac{1}{2}}$$

From an estimate of the errors in analytical concentrations as well as the rules for the propagation of errors it is possible to calculate a

limiting value of R, R_{lim}. If $R < R_{lim}$ the proposed model is regarded as being satisfactory.

The deprotonation curves (plots of Q as a function of pH) yield information which often complements that given by the formation curves. The deprotonation function Q is particularly useful in the representation of (i) ternary systems and (ii) regions of titrations where $\bar{Z}$ curves are ill defined (usually at high pH).

ESTA plots n, the average number of protons associated with each ligand molecule, as a solid line on the same graph as the deprotonation curve. This gives an estimate of the proton stoichiometry which predominates over a region of a titration.

ESTA also permits the calculation of the concentration of all species given their formation constants and the free or total concentration of each component. The distribution of components amongst all species is determined and can be presented graphically.

2.4 RESULTS AND INTERPRETATION

The protonation constant for maltol and the metal complex stability constants for aluminium, gadolinium and indium maltolates are given in Table 2.1.

2.4.1 Maltol

The protonation constant for maltol was determined to be 8.27. This value is in fairly good agreement with the literature valve, also indicated in Table 2.1, considering the different ionic strength (25 °C, 0.5M NaCl). This protonation constant is assigned to the only dissociable proton on the maltol molecule i.e. the hydroxyl proton.

The good agreement between the experimental and theoretical curves illustrated in Figure 2.2. allows us to have confidence in our experimentally determined constant. The Z-plot in Figure 2.2 is seen to rise to a limiting valve of 1 which confirms the fact that the ligand of interest has one dissociable proton.

Theoretical formation curves of $\bar{Z}_H$ vs pH for the protonation of maltol at 25°C and I = 0.15 M(NaCl).

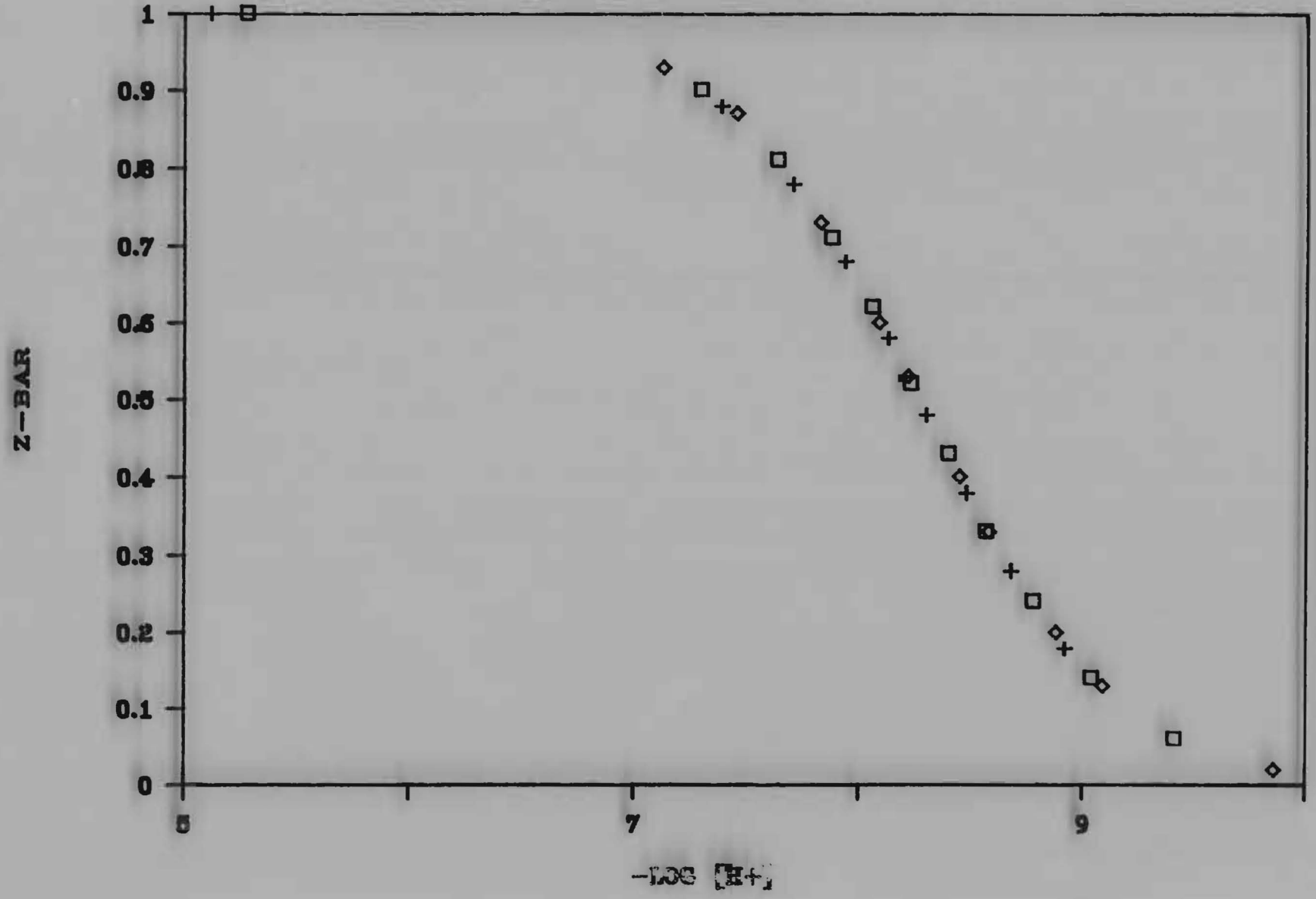

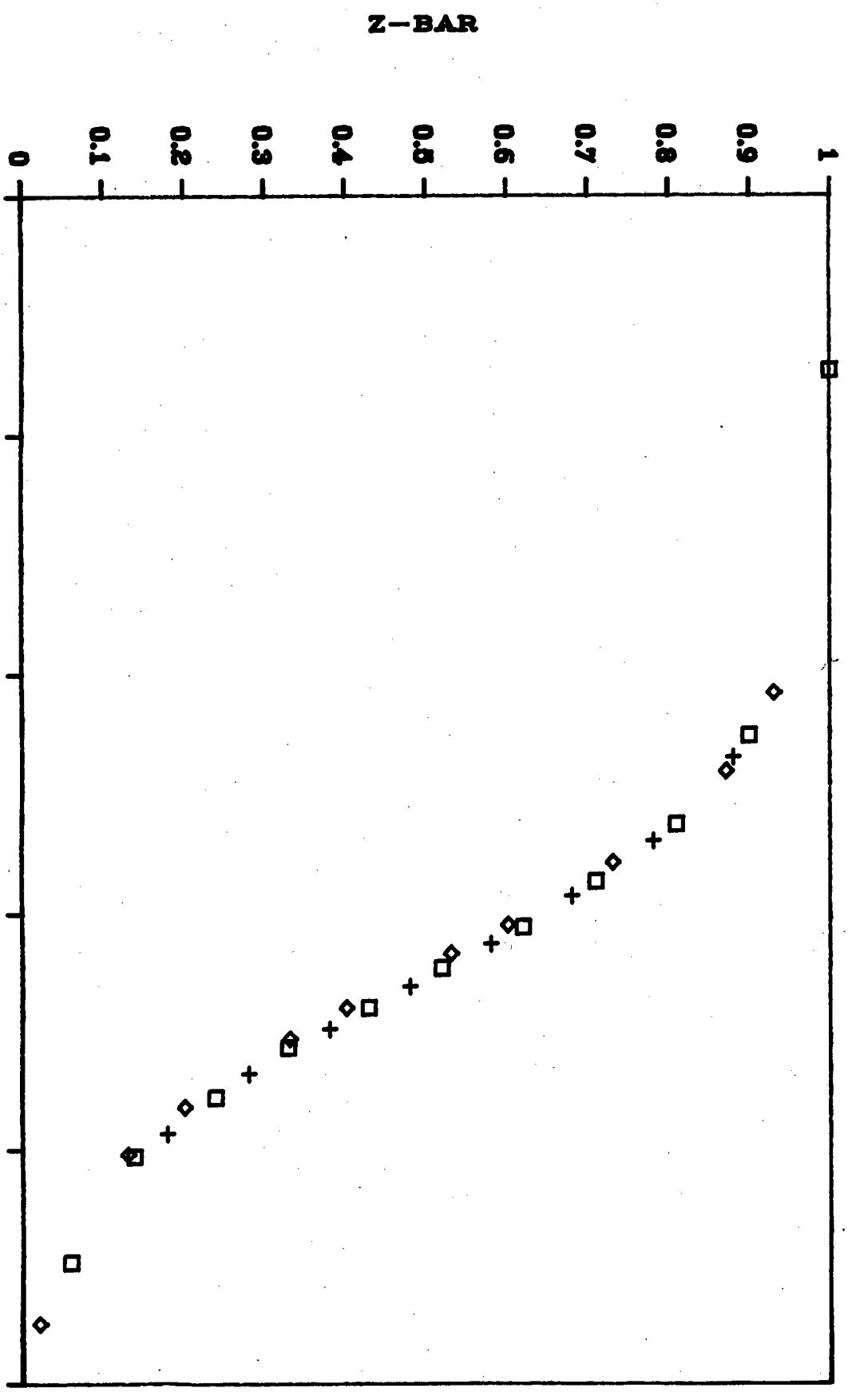

Figure 2.2 Experimental formation curves for $\bar{Z}_H$ vs pH for the protonation of maltol at 25°C and I = 0.15 M(NaCl).

2.4.1 Indium-Maltol

The indium formation curves in Figure 2.3 rise to a limiting valve of 2. This indicates that mainly InL and InL_2 complexes are formed over the pH range studied It was not possible to titrate to higher pH values due to the formation of precipitates. It should, however, be noticed that in the pH region considered, the formation curves appear to be independent of component concentration. Although no literature values of the indium maltolate complexes were available for comparison, the agreement between our experimentally determined curves and the pseudoplot curves suggest that the proposed model is acceptable. The inclusion of hydroxo species did not lead to an improvement of the Hamilton *R*-factor and were thus omitted from the model.

A species distribution curve, Figure 2.4, shows the variation of species concentration with pH.

Figure 2.3 Experimental formation curves of $\bar{Z}_M$ vs pA for the indium-maltol system at 25°C and I = 0.15 M(NaCl). The symbols represent different combinations of total ligand and total metal concentrations.

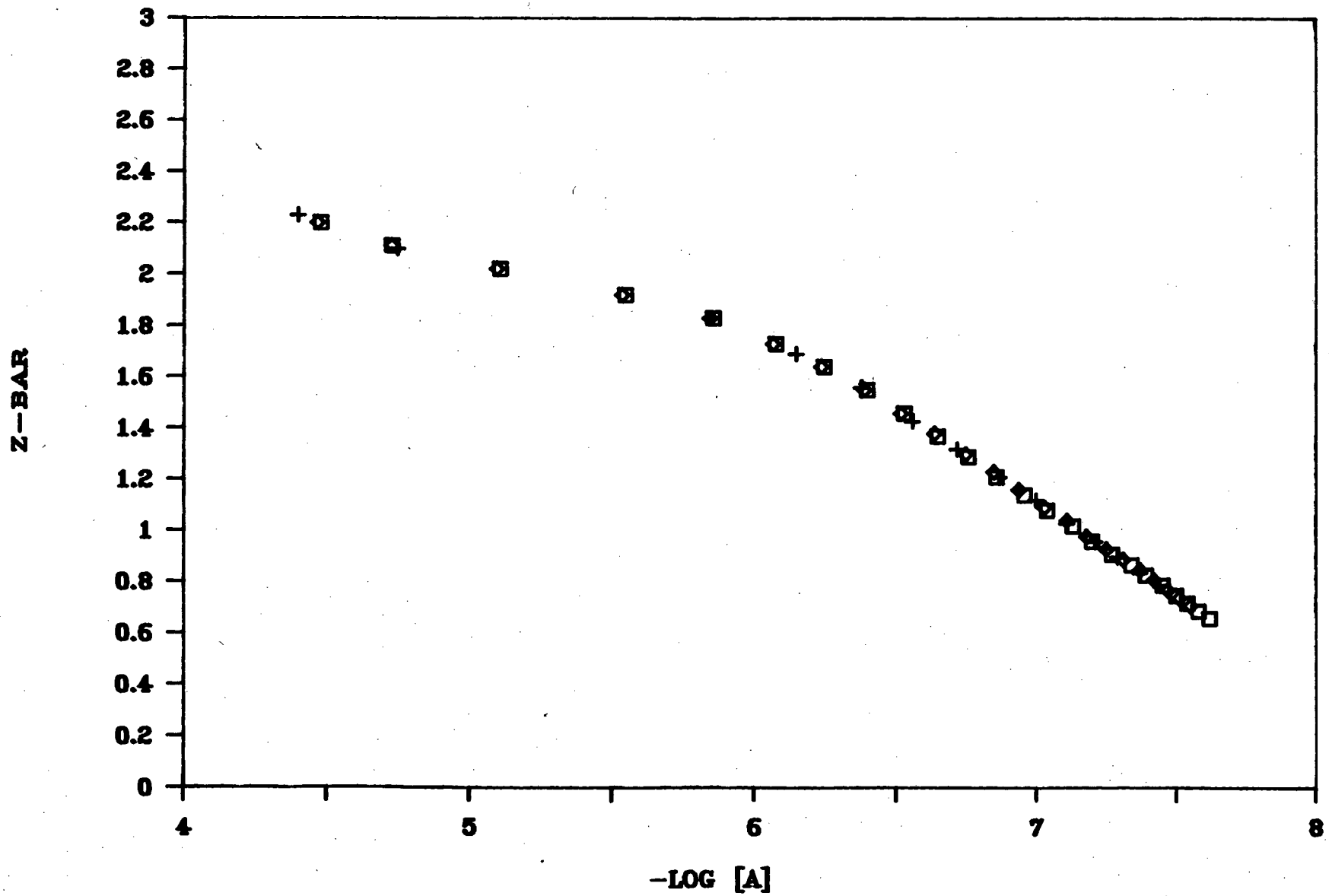

Theoretical formation curves of $\bar{Z}_M$ vs pA for the indium-maltol system at 25°C and I = 0.15 M(NaCl). The symbols represent different combinations of total ligand and total metal concentrations.

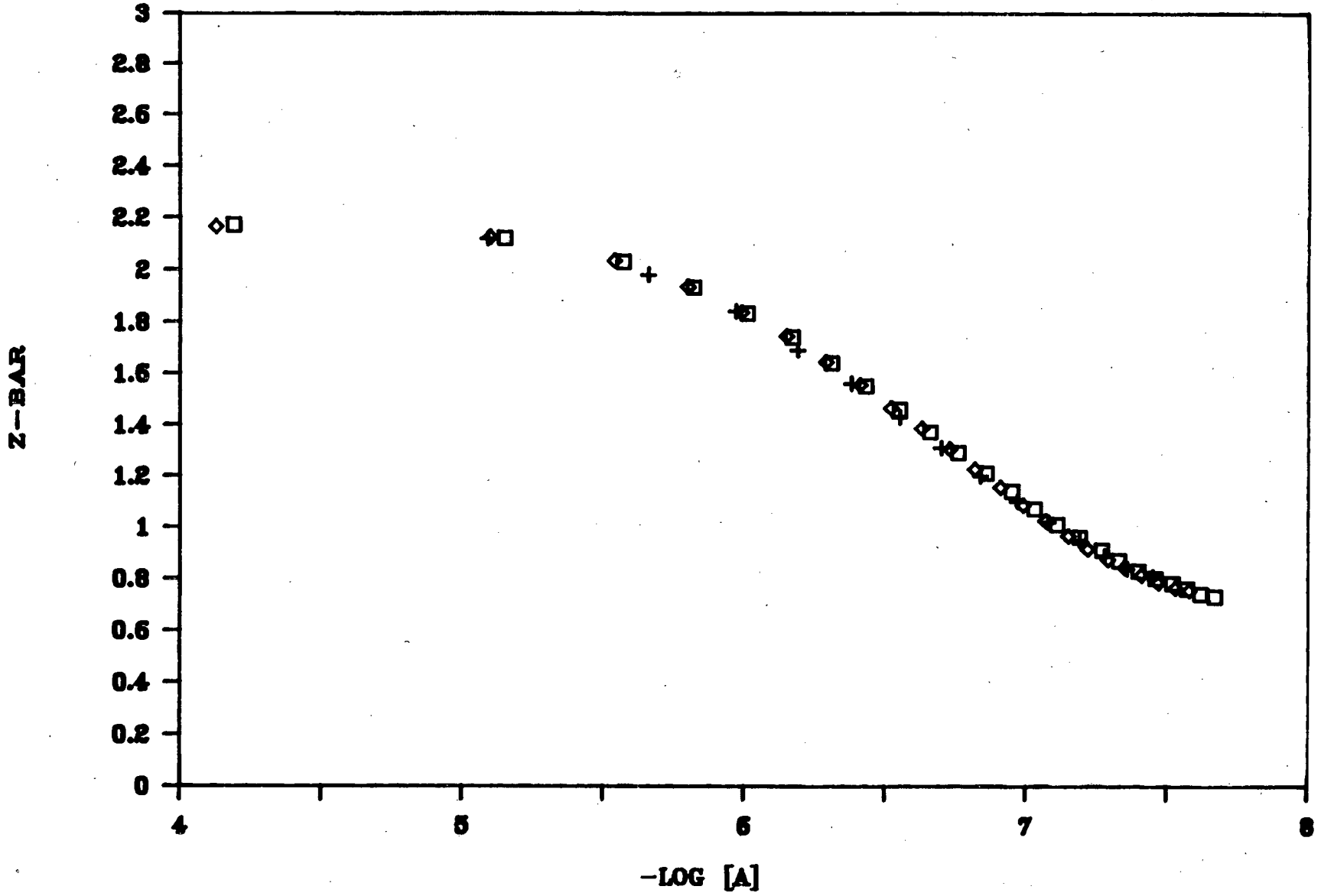

Figure 2.4 Species distribution curves for the indium-maltol system.

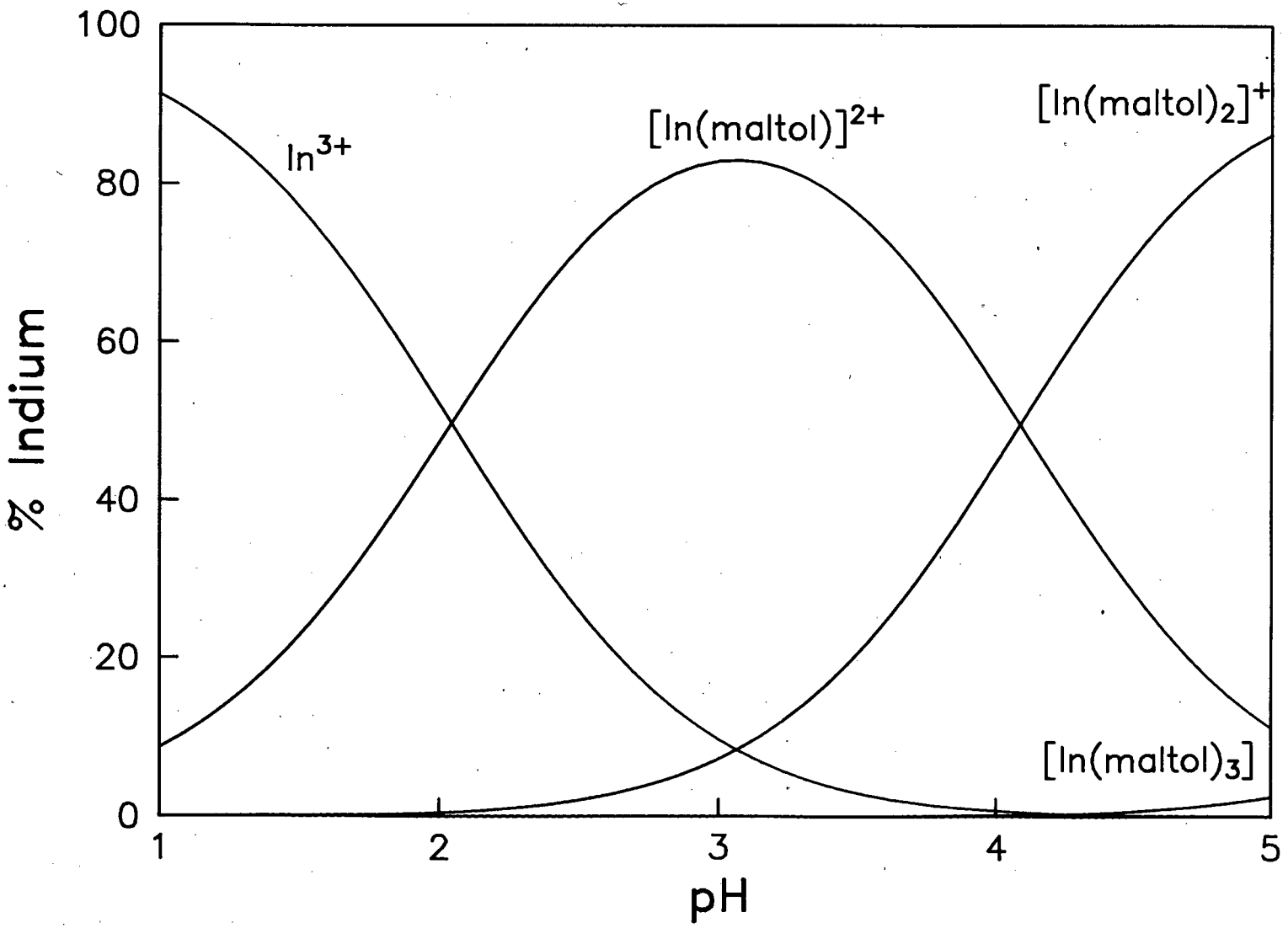

2.4.3. Aluminium-Maltol

From the $\bar{Z}$-plot of the Al(III)-maltol system (Figure 2.5) it can be seen that ML, ML_2, ML_3 species are formed under the experimental conditions used.

It should be noted that the curves do not drop to zero implying that complexation has already commenced at the start of the titration. The absence of fanning or back-bending indicated that, under the conditions of our experiments, no hydroxo- or polynuclear species were formed. Inclusion of such species in our model did not lead to an improved *R*-factor.

The agreement between theoretical (pseudoplot) and experimental curves give confidence to the β values determined. It should be noted that our β values are higher than those cited in the literature [7] even after taking into account the differences in ionic strengths and media.

A representative equilibrium species distribution diagram calculated for 4mM maltol and 1mM Al^{3+} is shown in Figure 2.6. It illustrates that the ML_3 complex becomes dominant at pH 4.5. Previously experiments [6] have demonstrated that the complex is stable to hydrolysis up to pH 9.

Theoretical formation curves of Z_M vs pA for the aluminium maltol system at 25°C and I = 0.15 M(NaCl). The symbols represent different combinations of total ligand and total metal concentrations.

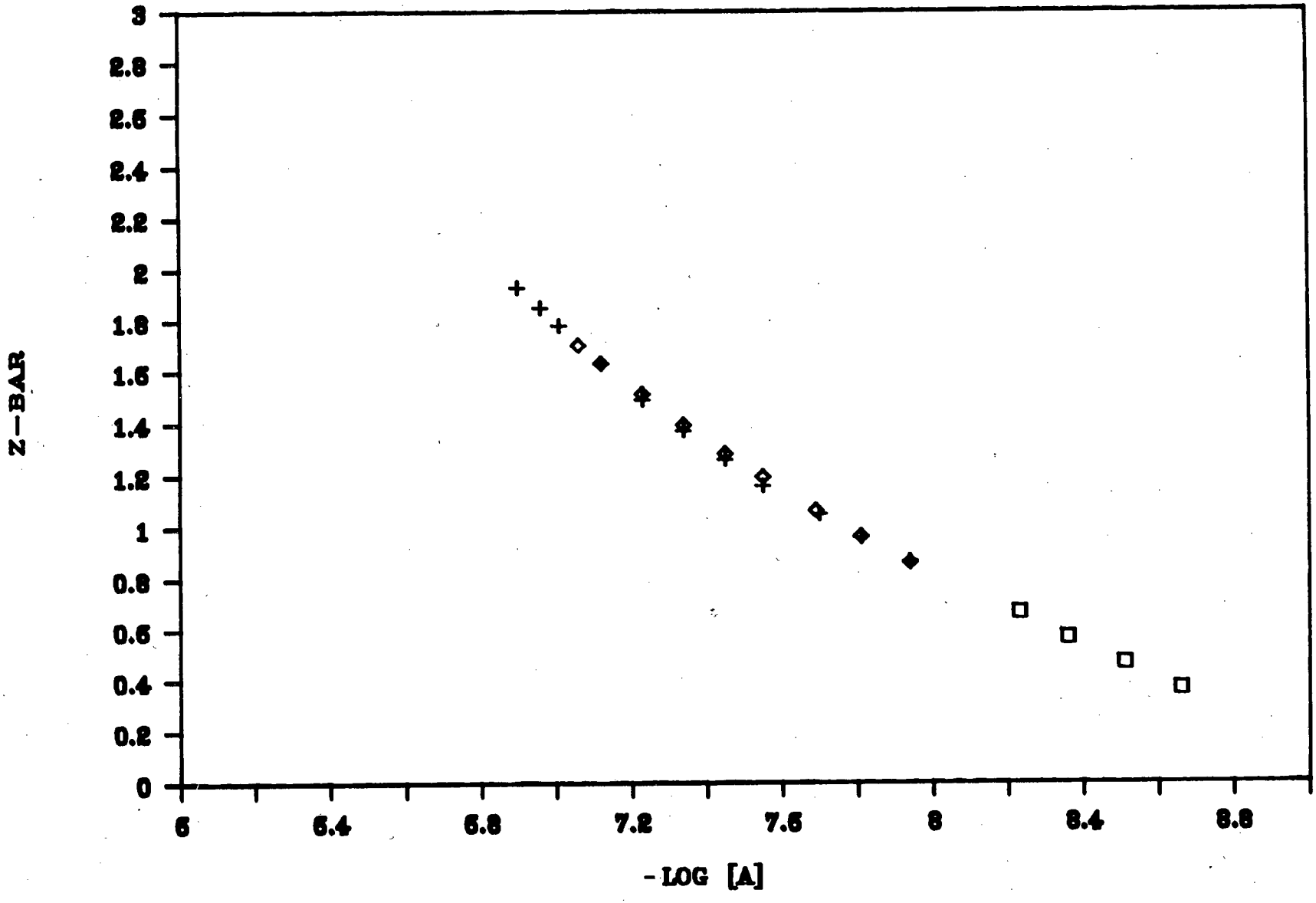

Figure 2.5 Experimental formation curves of Z_M vs pA for the aluminium-maltol system at 25°C and I = 0.15 M(NaCl). The symbols represent different combinations of total ligand and total metal concentrations.

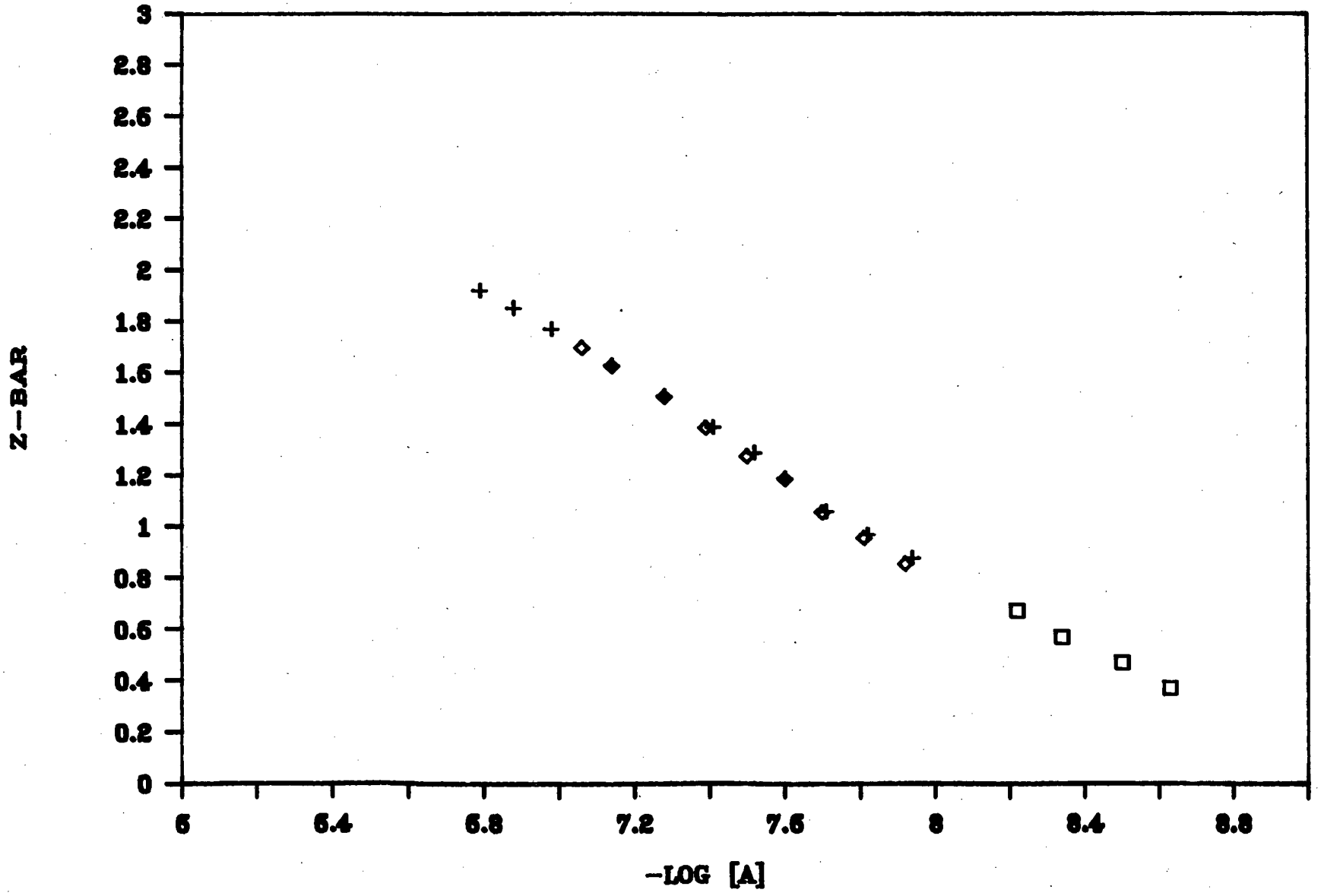

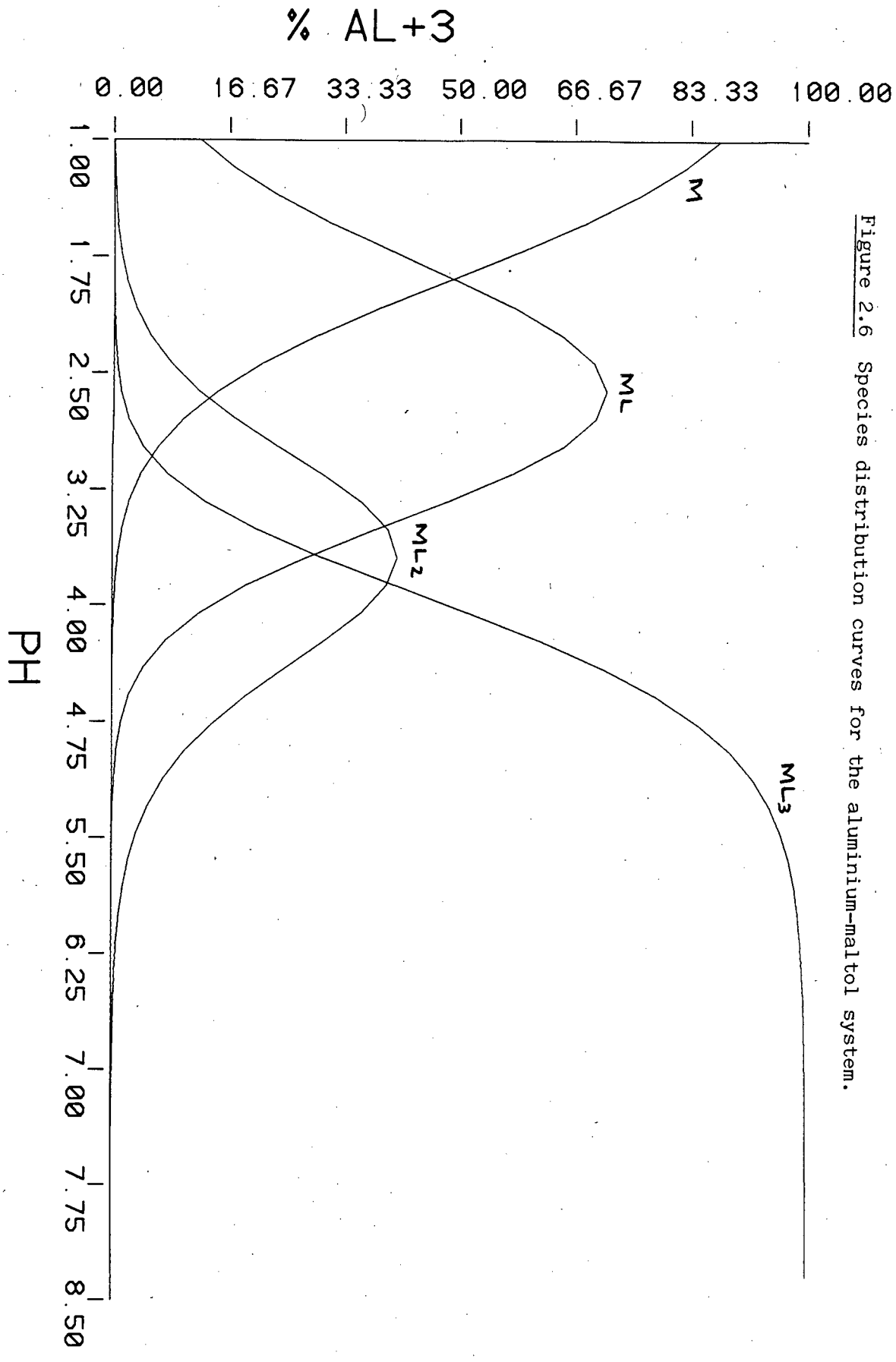

Figure 2.6 Species distribution curves for the aluminium-maltol system.

2.4.4 Gadolinium-Maltol

The metal-ligand stability constants determined for this system are significantly lower than those quoted in the literature. In spite of this, we have confidence in our proposed model because of the graphic agreement between theoretical and experimental Z-plots shown in Figure 2.7. No improvement to the model was obtained by the inclusion of any other species.

The Z-plots tend towards a value of 3 but never level off. This is because of the formation of a precipitate at higher pH. This data was discarded and not used in the refinement of the model.

The species distribution diagram in Figure 2.8 shows that even at pH 8.5, the ML_3 species is not fully formed.

Theoretical formation curves of Z_M vs pA for the gadolinium-maltol system at 25°C and I = 0.15 M(NaCl). The symbols represent different combinations of total ligand and total metal concentrations.

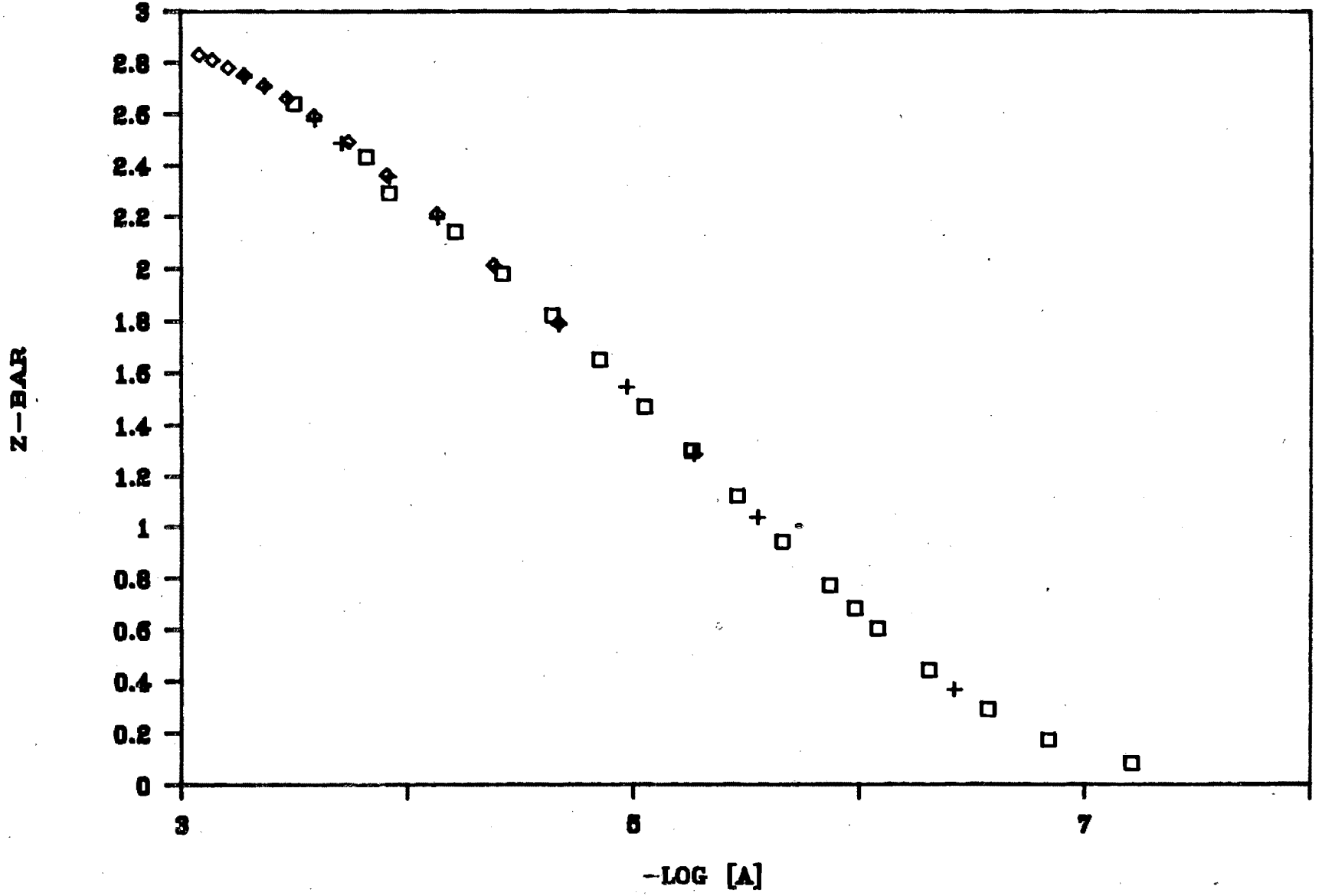

Figure 2.7 Experimental formation curves of Z_M vs pA for the gadolinium-maltol system at 25°C and I= 0.15 M(NaCl). The symbols represent different combinations of total ligand and total metal concentrations.

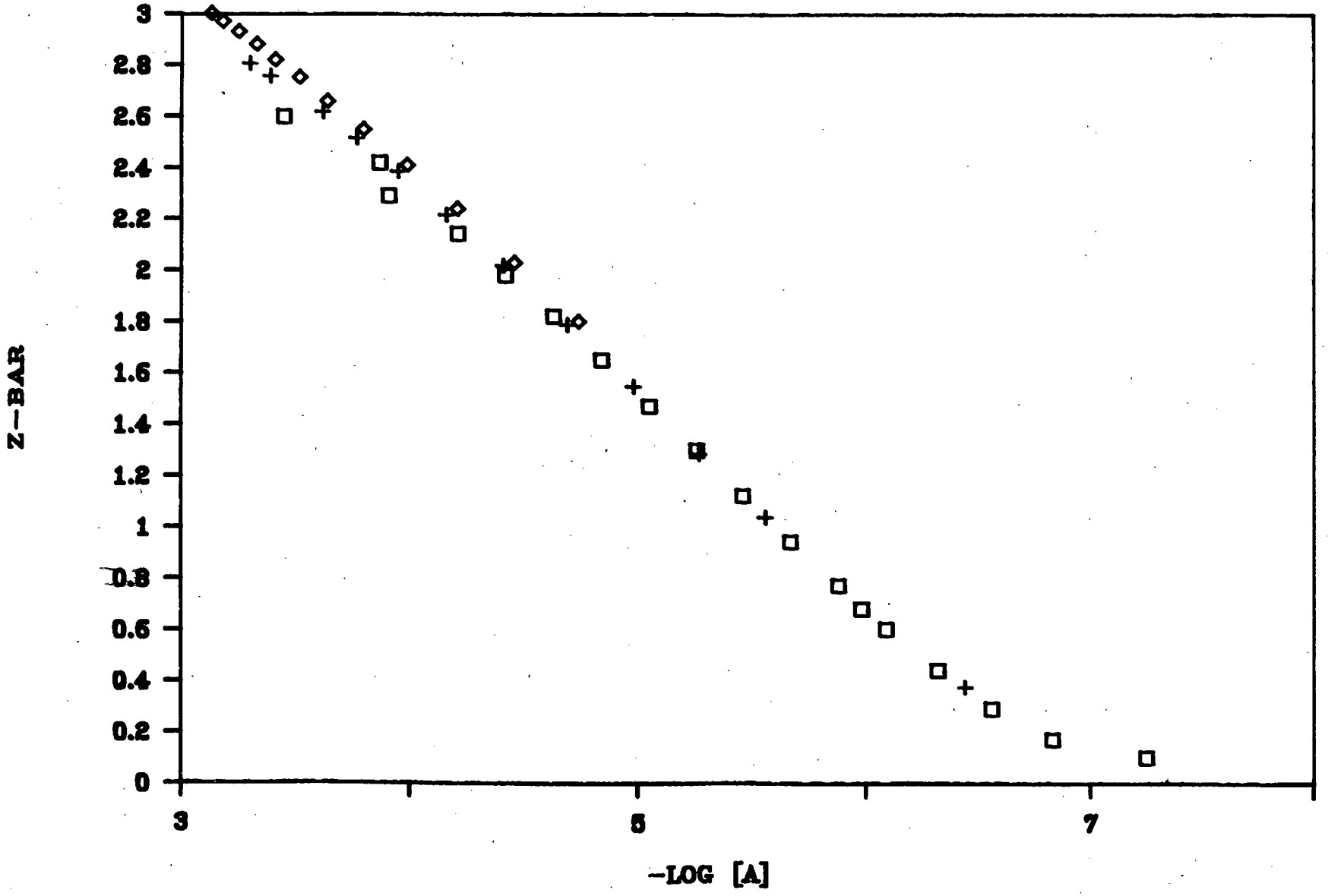

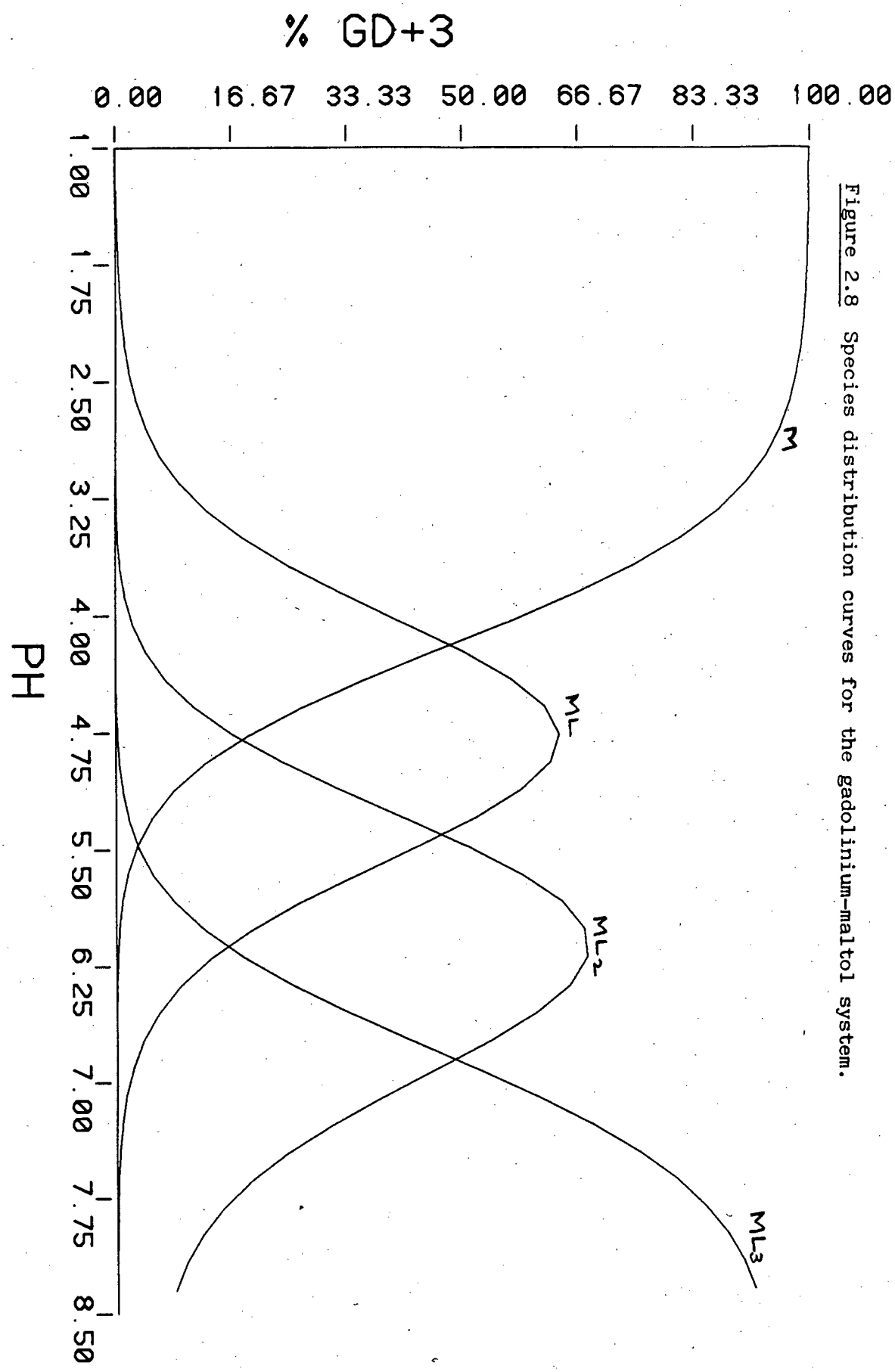

Figure 2.8 Species distribution curves for the gadolinium-maltol system.

Table 2.1 Logarithms of the maltol protonation constant and metal-ligand formation constants ($\log\beta_{pqr}$) as determined in this study at 25 ^{0}C and at ionic strength I = 0.15 M (NaCl).

Metal	p	q	r	$\log\beta_{pqr}$	R-factor	U	pH range
H^{+}	0	1	1	8.27 ±0.001 (8.36)	0.0013	9.02	5-9.8
In^{3+}	1	1	0	8.35 ±0.025	0.009	11.47	3-7
	1	2	0	14.72 ±0.033			
	1	3	0	18.67 ±0.099			
Al^{3+}	1	1	0	8.44 ±0.006 (7.7)	0.002	5.90	2-4
	1	2	0	15.54 ±0.01 (15.2)			
	1	3	0	22.16 ±0.039 (21.8)			
Gd^{3+}	1	1	0	6.14 ±0.006 (6.6)	0.007	3.92	3.4-8
	1	2	0	11.18 ±0.006 (11.9)			
	1	3	0	14.96 ±0.008 (15.8)			

a) The values in parentheses refer to values quoted by Martell A E and Smith M., Critical Stability Constants, vol3, Plenum Press, New York (1974).

2.5 DISCUSSION

Table 2.2 lists the protonation constants of maltol and other structurally similar ligands.

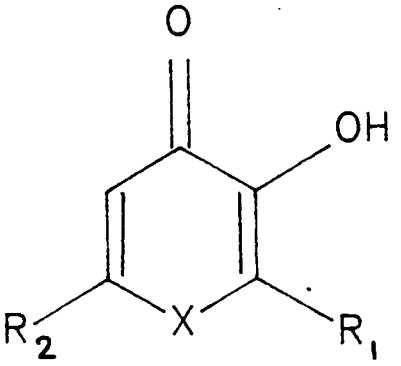

Table 2.2 Formation constants for a series of ligands structurally related to maltol.

R_1	R_2	X	$Log\beta_{011}$	$Log\beta_{110}$ Gd(III)	In(III)	Al(III)
H	H	O	7.69[a]			
CH_3	H	O	8.27[b]	6.15[b]	8.35[b]	8.44[b]
H	CH_3	O	7.94[a]			
H	CH_2Cl	O	7.43[a]	5.98[a]		
H	CH_2OH	O	7.66[a]	6.09[a]		
CH_3	H	NH	9.80[c]			11.87[c]
CH_3	H	NCH_3	9.86[c]			11.91[c]
CH_3	H	NC_2H_5	9.81[c]			11.75[c]
CH_3	H	NC_6H_{13}	9.92[c]			11.51[c]

a) Martell A.E. and Smith R.M., Critical Stability Constants, Plenum Press, New York.
b) This study.
c) Clevette D.J., Nelson W.O., Nordin A., Orvig C. and Sjoberg S., *Inorg. Chem.*, 28, 2079, 1989.

A comparison of the ligands listed in Table 2.2 indicates that the ligands containing a ring oxygen (3-hydroxy-4-pyrones) have lower protonation constants than the ligands containing a ring nitrogen (3-hydroxy-4-pyridinones). This suggests that the O-H bond is stronger in the 3-hydroxy-4-pyridinones. Charge delocalization occurs more readily

in the pyrones than the pyridinones and hence these ligands have lower pK_a's.

A trend which is evident for the hydroxy-pyridinones is that electron donating groups in the 2- and 6-positions tend to increase the ligand stability constant. The effect is more marked in the 2-position, which is *ortha* to the hydroxyl group. Such complexes would have a higher negative charge on the OH group than if an electron donating substituent was at the 6-position. Similarly, electron withdrawing groups such as CH_2OH and CH_2Cl lower the ligand stability constants.

Substitution at the ring N of the hydroxy-pyridinones has little effect on the ligand protonation and metal formation constants. This allows the properties of the metal-ligand complex, such as solubility and lipophilicity, to be varied without affecting thermodynamic stability. A new and interesting series of complexes of indium with hydroxy-pyridinones has been prepared [8]. These complexes were found to have a window of stability to hydrolysis around pH 4-9. This window is greater than that for the indium maltolates. The increased resistance to hydrolysis and the lipophilicity of these complexes has recommended their *in vivo* examination [9].

Comparison of $\log\beta_{110}$ for the Gd(III) maltolate complexes shows that these complexes are all of lower stability than their proton complexes. For In(III) and Al(III) $\log\beta_{110}$ is very similar to $\log\beta_{011}$. This maybe due to the charge density of the metal ions. In order to test this hypothesis $\log\beta_{110}$ of maltol is plotted (Figure 2.9) as a function of

ionic radius for a range of 3+ metal ions. Clearly as the charge density increases, ie the ion becomes smaller, the stability of the complex increases. Most of these metals are lanthanides and the typical consequence of the lanthanide contraction is seen with a break at Gd(III).

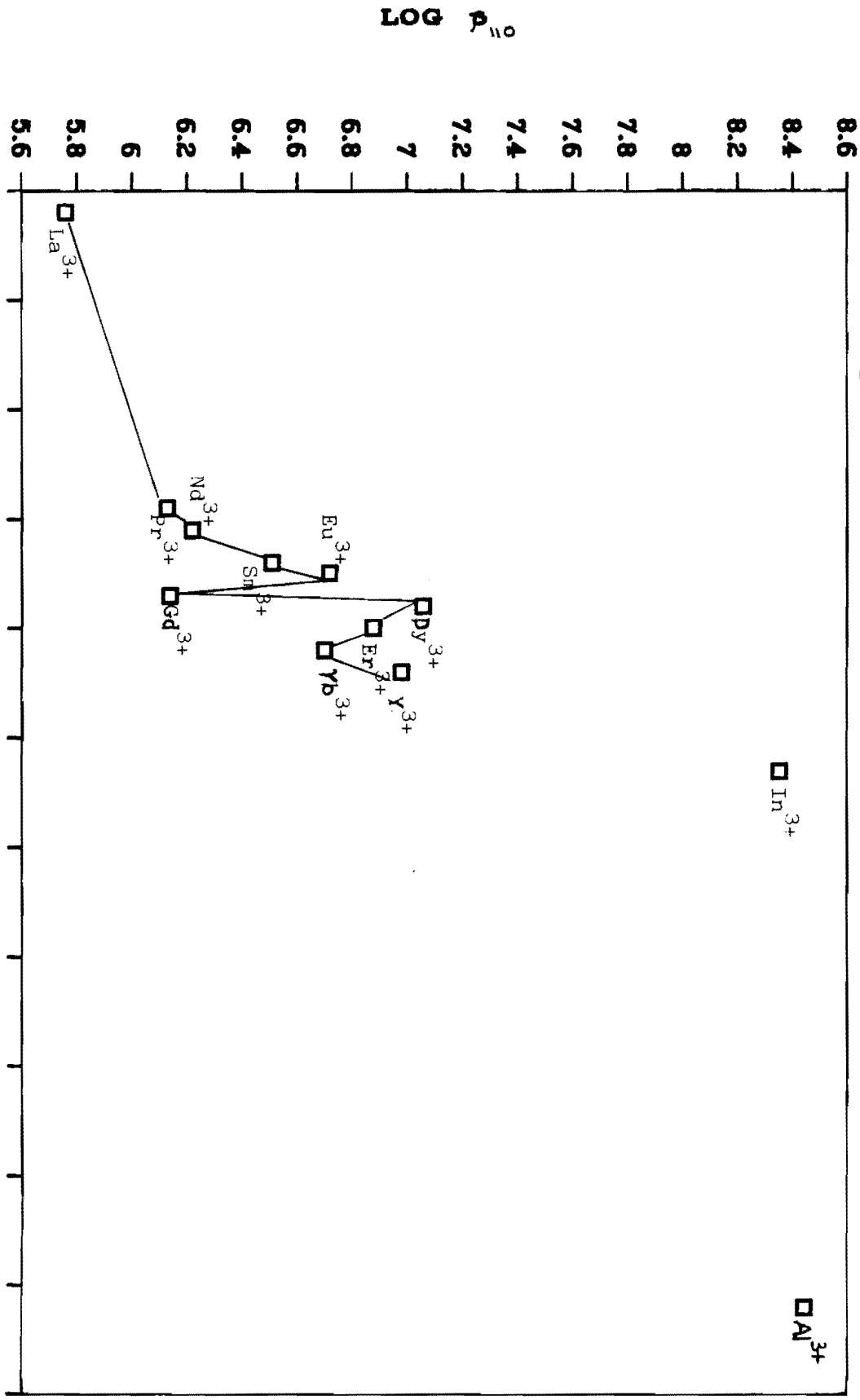

Figure 2.9 Plot of the logarithm of β_{110} for metal-maltolates against inverse metal^{3+} ionic radii.

REFERENCES

1. May P.M., Williams D.R., *Febs. Lett.*, 78 (1977) 134.

2. Vogel, A. *"Quantitative Inorganic Analysis"*, Longmans, 1961.

3. Gran G, *International Congress on Analytical Chemistry* 77,__(1952) 661.

4. Murray K, May P.M., *"Equilibrium simulation and Titration Analysis"*, Version 1.0., Univ. of Wales Institute of Science and Technology March, 1984

5. Vacca A., Sabatini A., Gristina M., *Coord. Chem. Rev.*, 8 (1972) 45.

6. Finnegan M.M., Rettig S.J., Orvig C.J., *J. Am. Chem. Soc.*, 108 (1986) 5033.

7. Martell A.E., Smith R.M., "*Critical Stability Constants*", vol. 1-4, New York, 1974-79.

8. Clevette D.J., Nelson W.O., Nordin A., Orvig C., Sjoberg S., *Inorg. Chem.*, 28, (1989) 2079.

9. Lutz T.G., Clevette D.J., Rettig S.J., Orvig C., *Inorg. Chem.*, 28, (1989) 715.

CHAPTER 3

NUCLEAR MAGNETIC RESONANCE STUDIES

3.1 INTRODUCTION

In 1939 Rabi *et al.* [1] sent a beam of hydrogen molecules first through an inhomogeneous magnetic field and then a homogeneous field, and they applied radio-frequency electromagnetic energy to the molecules in the homogeneous field. At a specific frequency, energy was absorbed by the molecular beam and caused a small but measurable deflection of the beam. This was the first actual observation of nuclear magnetic resonance. It was not until 1946 that Bloch [2] at Stanford and Purcell [3] at Harvard discovered nuclear magnetic resonance (NMR) in bulk material.

NMR attracted little attention from chemists until 1949 and in 1950 it was discovered that the precise resonance frequency depends on the state of its chemical environment. This discovery of chemical shift provided the necessary impetus for the use of NMR as a probe for molecular structure. In the 30 years that have elapsed since the chemists discovery of NMR spectroscopy, the technique has proved to be a powerful and informative technique for analytical, structural and dynamic investigations of all forms of matter. Besides the field of chemistry, the fields of physiology, biochemistry, and medicine are also finding vast applications of NMR spectroscopy.

The fundamental principles of NMR have been dealt with in a number of standard texts [4,5]. Only the aspect of NMR which are relevant to the present study will be discussed in this thesis.

3.2 THE NMR DETERMINATION OF PROTONATION CONSTANTS

Although the protonation constants of organic ligands are generally determined by potentiometry, it is often not possible to unambiguously assign the sites of protonation by the latter method, particularly if the ligand of interest has more than one protonation site. The ligands EDTA and DTPA are examples of the latter case. With the aid of NMR spectroscopy, the assignment of the protonation constants to various protonation sites becomes a trivial task. Chan *et al.* [6] ascertained the protonation characteristics of DTPA by analogy with those of EDTA by studying the chemical shifts of DTPA as a function of solution pH. It is not possible to study EDTA protonation directly by this method as the H_4EDTA species precipitates when further protonation occurs.

The chemical shift of nuclei closest to the protonation site are most sensitive to changes in pH, particularly in a pH region near the pK_a of a ligand.

By plotting chemical shift as a function of pH for the various resonance of an organic ligand, the pka value as well as the site of protonation can be determined. As a first approximation the pK_a is equal to the pH at the point of inflection.

Although there is no ambiguity in the assignment of the protonation constant of maltol, as there is only one dissociable proton situated on the hydroxyl group attached to the ring, NMR studies are still of use in confirming the protonation constants determined by other techniques.

3.3 NMR OF METAL COMPLEXES

NMR has proved to be a useful technique for studying both diamagnetic and paramagnetic complexes [7,8]. The NMR spectrum of the ligand may give useful information about the structure of the complex in solution. On the other hand, because of exchange between the various possible isomers of the complex, the interpretation of the spectra is generally more complex.

The first quantitative theory of chemical exchange in NMR was developed in the classic paper of Gutowsky *et al.* [9]. Based on this approach we can consider the equilibrium ML = M + L (where M is a diamagnetic metal and L an organic ligand) If the exchange is very slow, as is often the case when M = Al^{3+}, then two independent spectra are likely to be seen. One characteristic of the free ligand and the other characteristic of the complex.

If ML = L + M exchange is very rapid, as is often the case when M = In^{3+}, essentially none of the nuclei will behave in a manner which is characteristic of either ML or L as very few nuclei will have been in either environment long enough to reflect its characteristics. Essentially the nuclei behave in a manner which is an average of the two environments. Because of this phenomenon, the NMR spectrum will

consist of a single set of peaks, the position and width of which are the weighted average of the free and complexed ligand.

3.4 NMR OF PARAMAGNETIC SYSTEMS

It is well known that a perturbed nuclear spin system relaxes to its equilibrium state by first order processes characterised by two relaxation times: T_1 the spin-lattice or longitudinal relaxation time; and T_2 the spin-spin or transverse relaxation time.

A great deal of chemical information can be obtained by studying the relaxation processes. Of particular interest in the current study is the contribution of paramagnetic metal atoms to the relaxation of nuclei. Relaxation by a paramagnetic agent can be brought about in two ways (i) contact interactions and (ii) pseudocontact interactions. The basic equations for relaxation of a paramagnetic agent were derived by Solomon [10] and Bloembergen[11]. Contact interactions involve the transfer of unpaired electron density to the relaxing atom itself. Pseudocontact interactions arise from the magnetic dipolar fields experienced by a nucleus near the paramagnetic ion.

Both contact and dipolar shifts from unpaired electrons are temperature dependent, normally varying approximately as 1/T. The rapid nuclear relaxation caused by the presence of unpaired electrons leads to line widths substantially greater than those expected from spin-lattice relaxation.

The field experienced by one nuclear moment and caused by another of magnitude m is proportional to m/r^3. A given nucleus experiences a field of this magnitude from each of the surrounding nuclei, and each such contribution will either augment the field applied to a sample or detract from it, depending on the alignment of each magnetic moment with respect to the applied field. Since all the nuclei do not experience the internuclear field, the resonance frequencies of the nuclei will differ and the observed spectral line will be broadened.

The large chemical shifts caused by certain paramagnetic species (particularly the lanthanide elements) have been exploited in shift reagents. These reagents contain a paramagnetic ion attached to a ligand that can in turn complex with the molecule being studied [12]. For instance the normal spectrum of pentanol is found low field of TMS and consists of a triplet due to the methylene protons adjacent to the alcohol group and two groups containing a series of overlapping lines due to the remaining protons which all have very similar chemical shift. If a praseodymium complex is added to the solution all the resonances move upfield and become sufficiently separated to give first-order spectra. Alternatively if a europium complex is used the contact shift is downfield.

In addition to the paramagnetic agents which affect the chemical shift of a nucleus, there is a class of paramagnetic metals which broaden an NMR spectrum. This broadening effect is related to the individual electron-spin relaxation times.

For the 'broadening' metal ions like Mn^{2+} and Gd^{3+} the degree of broadening is given by Equation (3.1)

$$\Delta\nu_{\frac{1}{2}} = 1/\pi T_{2p} = (f/15\pi)(\gamma_I^2 g^2 \beta^2 s(s+1))/r^6 \cdot 7\tau_c \quad \ldots\ldots (3.1)$$

where $\Delta\nu_{\frac{1}{2}}$ is the width at half height

r is the metal-proton internuclear distance

f is the mole fraction of bound ligand and

τ_c the correlation time modulating the interaction

The other symbols have their usual significance.

Since $\Delta\nu_{\frac{1}{2}}$ can be measured directly from the spectrum, it is theoretically possible to calculate the metal ion-proton internuclear distance. In practice the accurate determination of τ_c is often difficult. For this reason relative internuclear distances are calculated rather than absolute internuclear distances. This is done by determining the broadening produced by differing metal concentrations. A plot of $\Delta\nu_{\frac{1}{2}}$ against f should then yield a straight line with slope $1/r^6$.

This relation is described in Equation (3.2)

$$(r_A/r_B)^6 = (\text{slope})_A/(\text{slope})_B \quad \ldots\ldots (3.2)$$

where A and B denote ligand protons.

3.5 THE USE OF OTHER MAGNETIC NUCLEI

Because of the very large number of organic compounds studied by chemists, ^{1}H and ^{13}C spectra are the most commonly encountered. There are many other nuclei which are magnetically active and that have found increasing application as multinuclear, high field spectrometers, have become more widely available.

^{13}C NMR

Although the natural abundance of ^{13}C is only 1.1%, the high resolution spectra corresponding to the ^{13}C nuclei are routinely studied. Direct information on carbon atoms which are not attached to hydrogen atoms, such as carbonyl groups is possible. In this way ^{13}C spectroscopy has greatly increased the scope of NMR.

^{27}Al NMR

^{27}Al NMR is being used extensively to study the interactions occurring in ionic solutions since the rates of exchange around the triply charged cations are relatively slow and separate species can often be observed.

The hydrolysis of several aluminium complexes has been studied using ^{27}Al NMR [13,14].

In addition to the NMR techniques discussed there are a large number of new experimental techniques which have developed in recent years and which are proving to be useful not only to the chemist, but also in the fields of biochemistry, medicine and physiology.

3.6 EXPERIMENTAL

Reagents: Deuterium oxide (99.86 %) was used as solvent for all the NMR studies. All other reagents used were as described in Chapter 2.

Instrumentation: All NMR spectra were recorded on a VXR200 spectrometer at a probe temperature of 23 ^{0}C. pH Measurements were made at ambient temperature using a Radiometer pH meter. No correction was made for the difference in activity of deuterium and hydrogen ions.

Ligand-protonation study: The ligand protonation constant was determined from data obtained from NMR spectra of 0.1 *M* ligand solution recorded at different pH. The ligand solution pH was varied by the addition of NaOD.

Metal-ligand studies: Gadolinium titrations were carried out on 0.1 *M* ligand solutions. A μ-syringe was used to make small additions of metal stock solution to the ligand solution. The spectrum of the ligand was recorded after each addition and the line-broadening monitored by measuring $\Delta\nu_{\frac{1}{2}}$, the width at half-height of the resonances in the ^{1}H spectra.

The indium and aluminium-maltol systems were studied by recording ^{1}H nmr spectra of maltol solutions, at a metal:ligand ratio of 1:3, over the pH range 3 - 9.

3.7 RESULTS AND DISCUSSION

The chemical shifts in the ^1H spectra are referred to TPS (triphenylsilyl propanealphonic acid, sodium salt) as zero. A representative spectrum of maltol is illustrated in Figure 3.1, which consists of two *AB* doublet patterns centred at δ6.26 and δ7.74 and a singlet at δ2.15. Based on literature chemical shifts, the spectrum was assigned as indicated in Table 3.1.

Table 3.1 Chemical shifts and assignments for 0.1 *M* maltol in D_2O at 25 °C.

Chemical Shift	Assignment
1.78 singlet	CH_3
6.26 doublet	H-5
7.74 doublet	H-6

The above assignment are in agreement with those indicated in the literature [15] but the actual chemical shift values differ considerably. The OH proton is not observed due to rapid exchange of this proton with the deuterium from the solvent.

Protonation of Maltol

The change in chemical shifts accompanying the change in pD is shown in Figure 3.2. It can be seen from this curve that between pD 7.8 and 9.8 the chemical shift is very sensitive to change in pD. Between pD 5 and 7.8 the chemical shifts tend to be fairly constant while beyond pD 7.8

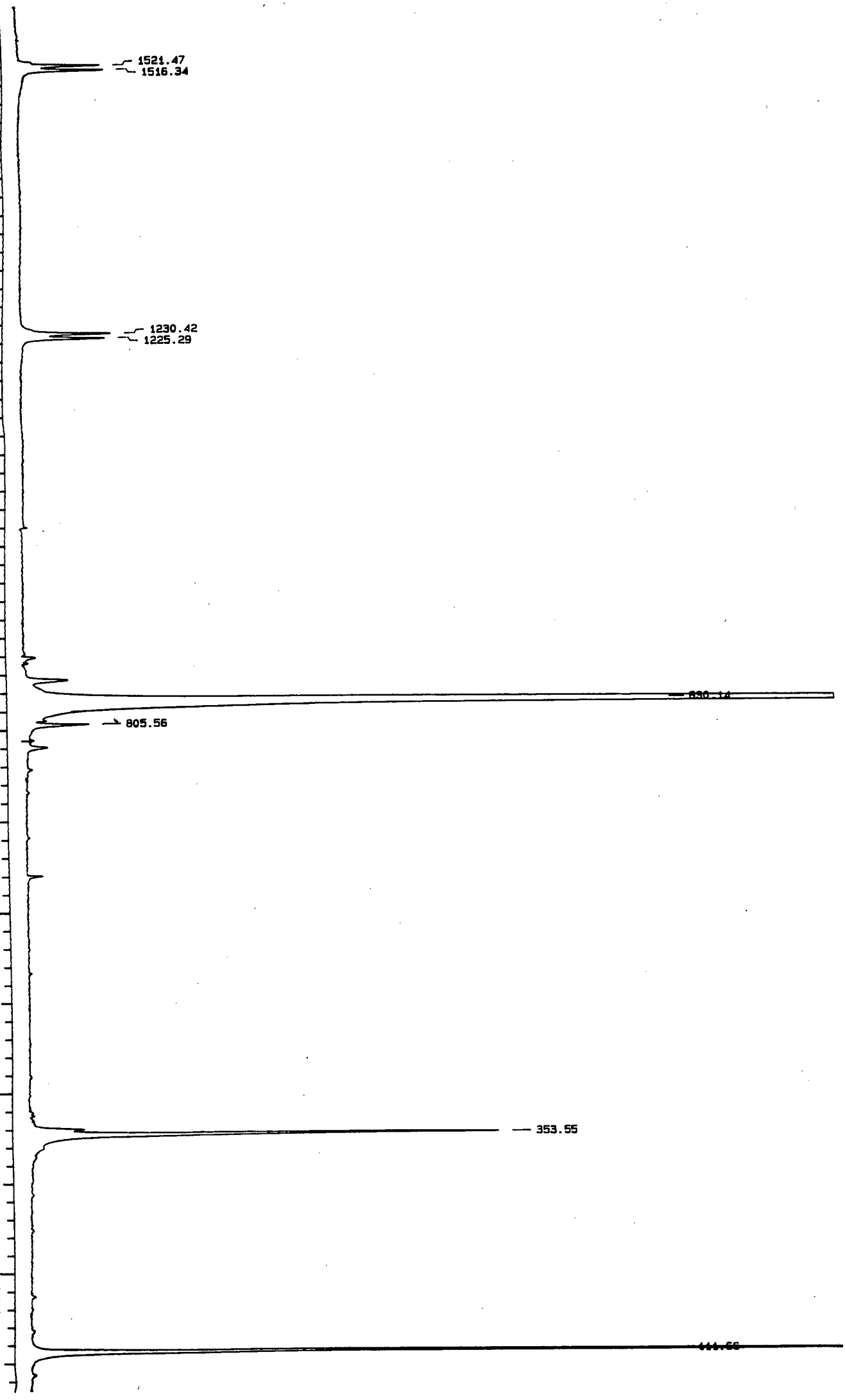

Figure 3.1 ^{1}H NMR spectrum of maltol.

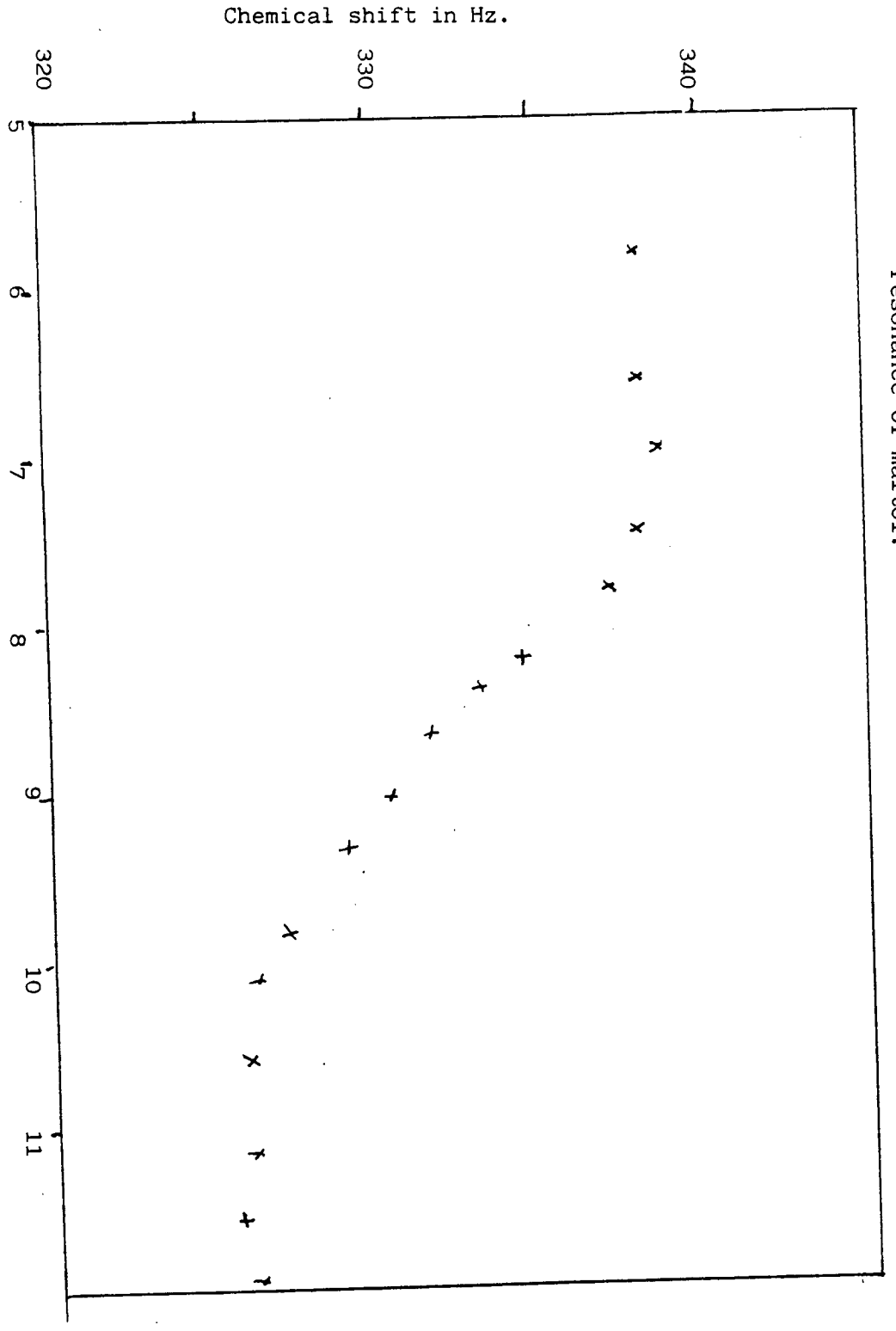

Figure 3.2 Plot of chemical shift against pH for the CH_3 resonance of maltol.

Figure 3.3 Spectral changes in the ^{1}H spectrum of maltol as a function of pH.

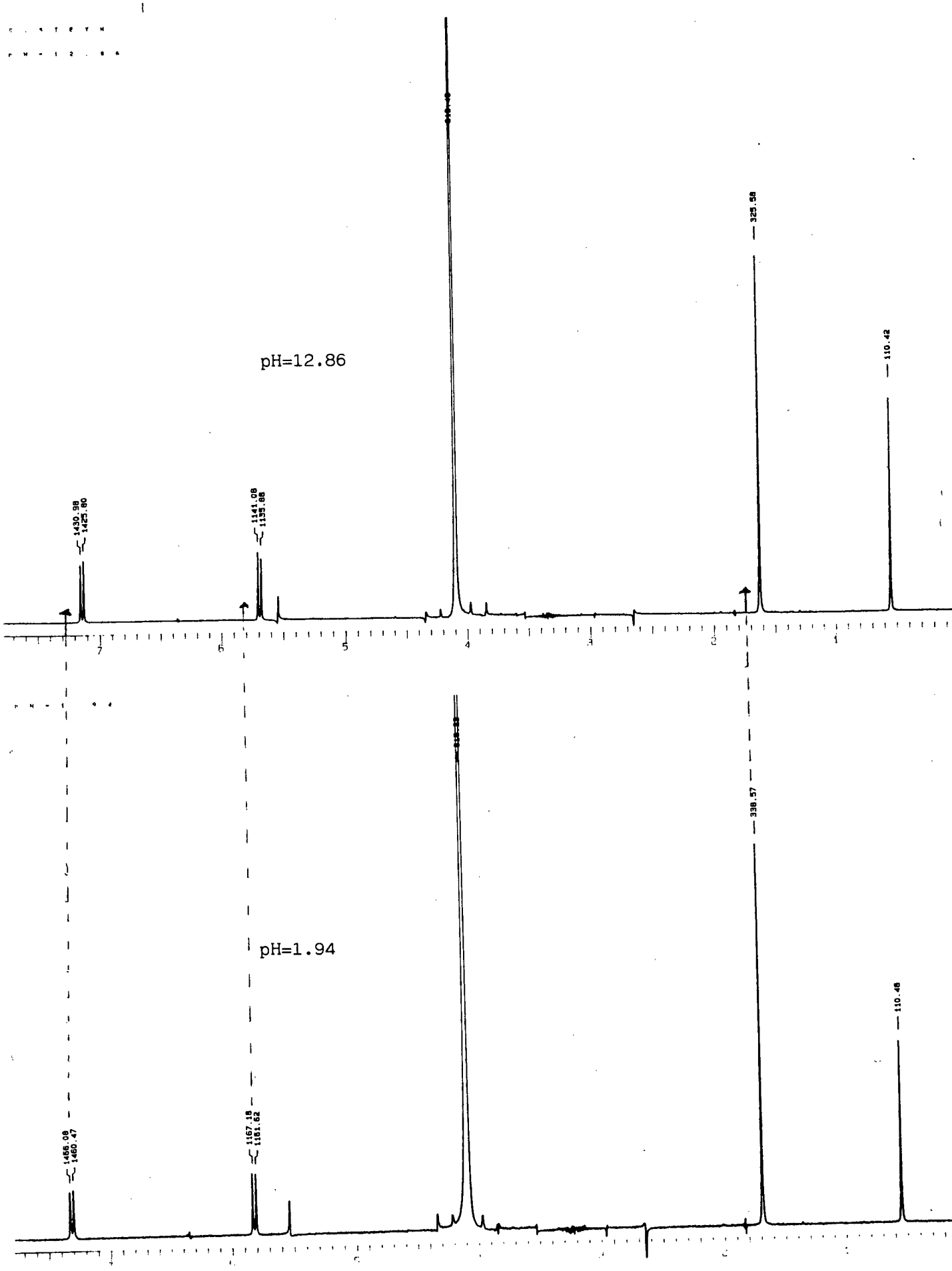

change rapidly with increasing pD. Beyond pD 9.8 the chemical shifts again become almost independent of pD.

From the point of inflection of the curve the pK_a of maltol is estimated to be 8.35 (applying correction pD = pH + 0.4). This value is in reasonable agreement with the pK_a determined potentiometrically (Chapter 3).

Figure 3.3 shows the spectral changes in the proton spectra of maltol as a function of pH.

Maltol-Gadolinium system

Figure 3.4 shows the effect of gadolinium on the proton spectrum of maltol. It can be seen from these data that the effect of Gd^{3+} on the TPS resonance is much less than the effect on the maltol resonances and represents the change in bulk susceptibility of the solution. The differential broadening of the maltol resonances is due to the fact that those nuclei closest to the metal ion are preferentially broadened. In this way paramagnetic metal broadening agents can be used to assign NMR spectra of more complex ligands than maltol. Alternatively from known assignments it is possible to use the preferential broadening to calculate the position of the metal ion in the complex. This is shown in Figure 3.4.

Figure 3.4 The effect of Gd^{3+} on the ^1H NMR spectrum of maltol

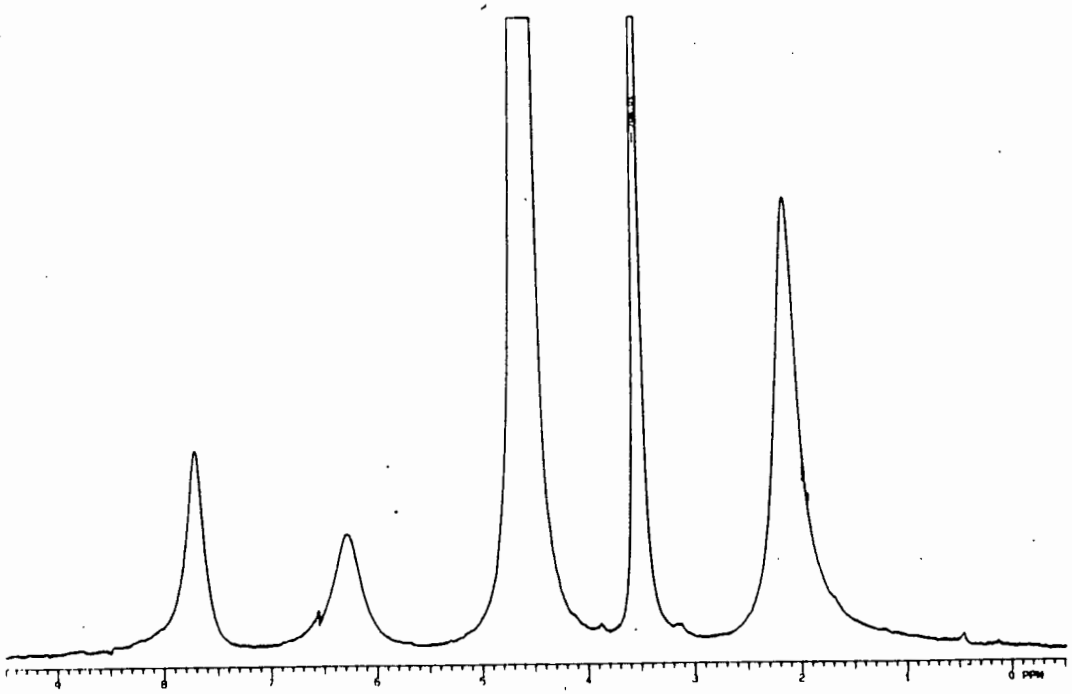

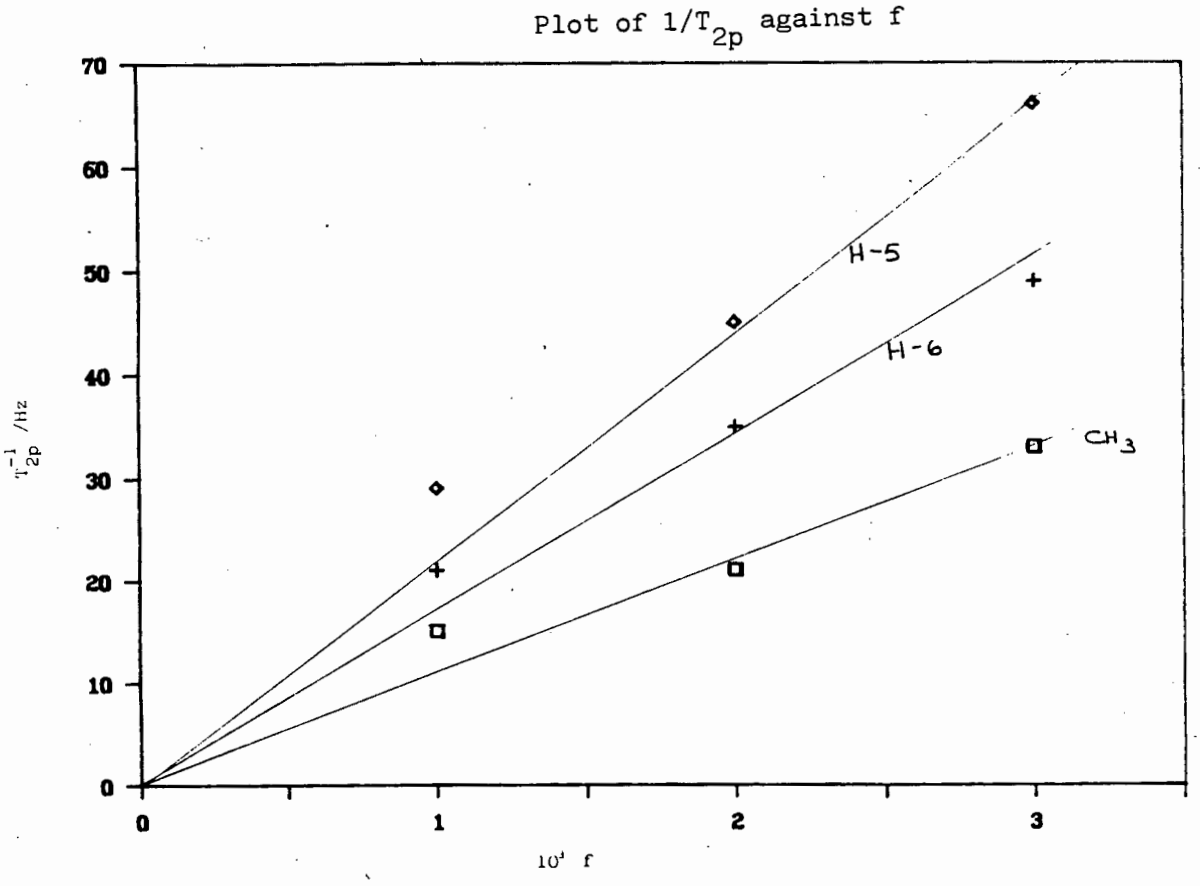

Experimentally determined proton-metal distances for maltol-Gd(III) system.

Proton	Experimentally determined distance[a]
CH_3	1.4
H-5	1.0
H-6	1.2

(a) relative to H-5

Maltol-Indium system

It was not possible to record the ^1H NMR spectra of indium-maltol solutions at pH values greater than 2, due to the formation of a precipitate. It was not practical to further dilute the solutions as we were already working at the minimum practical ligand concentration to obtain ^1H NMR spectra. Elemental (C,H,N) analysis of the precipitate was consistent with the formation of $In(maltol)_3 \cdot H_2O$.

Maltol-aluminium system

The ^1H NMR spectrum of this system showed interesting spectral changes as the pH increased. As the pH was increased from 1.3 to 1.8, the appearance of a new set of resonance lines was observed (see Figure 3.5). As the pH was further increased these resonance lines changed in intensity and other resonance lines started to appear.

The appearance of this different set of signals is indicative of the fact that complexation between maltol and aluminium is occurring and that the exchange ML = M + L is slow on the NMR time scale. It was not possible to assign the spectrum of the complex.

^{27}Al NMR

The results of a variable pH ^{27}Al NMR studies of a solution containing aluminium and maltol ([M] << [L]) is shown in Figure 3.6. At pH 1.4 the presence of $[Al(H_2O)_6]^{3+}$ is seen. ^{27}Al, which has a quadrupole moment generally gives rise to very broad signals. In a very

Figure 3.5 ^{1}H NMR spectra of aluminium-maltol system recorded at various pH.

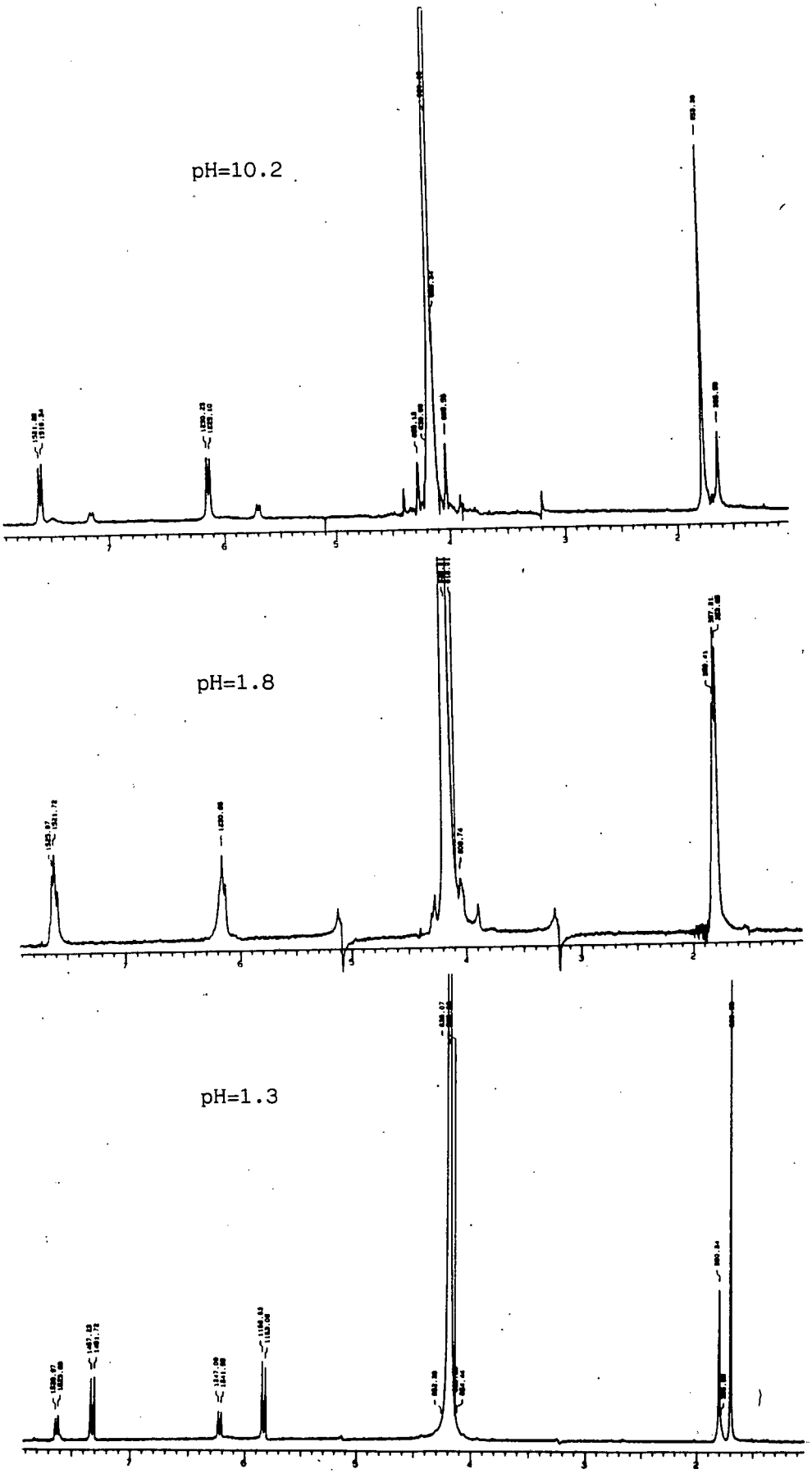

symmetrical electronic environment, however, sharp peaks are often seen as is the case for $[Al(H_2O)_6]^{3+}$. The broadness of an ^{27}Al resonance can in fact be used as a good indication of the symmetry of the coordination sphere of the metal ion. As the pH is raised Al(III) maltol complexes are formed. The intensity of the $[Al(H_2O)_6]^{3+}$ decreases and is replaced by much broader peaks due to the Al(III) maltol complexes. It is not possible to resolve the single broad peak into peaks due to the individual Al(III) maltol species. It maybe that, because of the large electrical field of the unsymmetrical $[Al(maltol)]^{2-}$ and $[Al(maltol)_2]^-$ complexes the signals due to these two complexes are so broad as to not be seen at all. Above pH 9 the $[Al(maltol)_3]$ complex hydrolyses to $[Al(OH)_4]^-$ as is indicated by the sharp peak in Figure 3.6.

A representative equilibrium species distribution diagram calculated for 5 mM maltol and 1 mM Al^{3+} is shown in Figure 3.6. This diagram supports the conclusions drawn from the ^{27}Al NMR spectra.

Figure 3.6 a ^{27}Al NMR of aluminium-maltol system recorded at various pH.

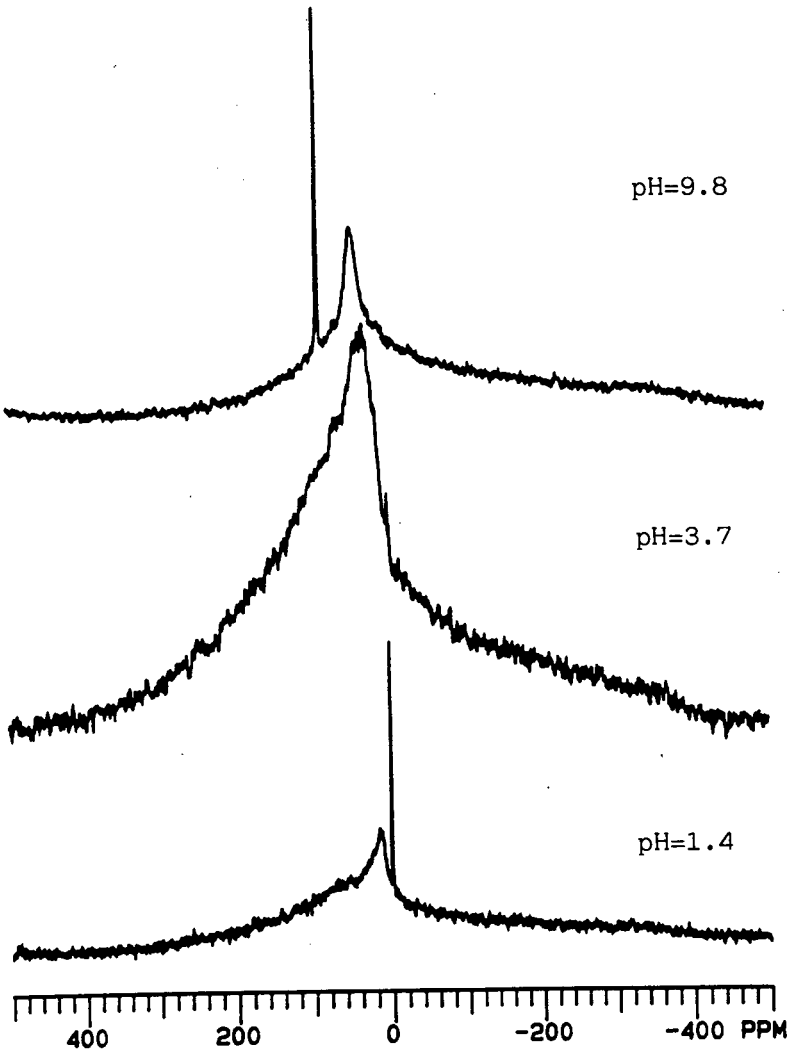

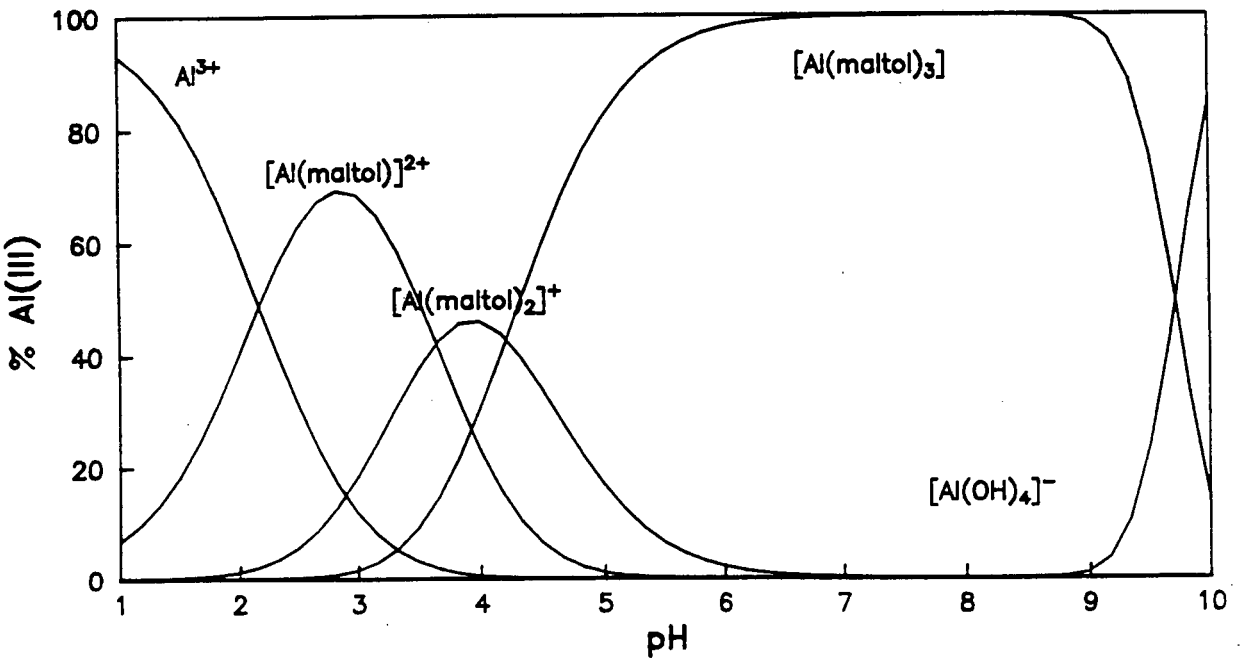

Figure 3.6b A representative species distribution diagram for the aluminium-maltol system.

REFERENCES

1. Rabi I., Millman S.,Kasch P., Zacharius J.R., *Phys. Rev.*, **55** (1939) 526.
2. Bloch F., Hansen W.W., Packard M., *Phys. Rev.*, **69** (1946) 127.
3. Purcell E.M., Torrey H.C., Pound R.V., *Phys. Rev.*, **69** (1946) 37.
4. Roberts J.D., "Nuclear Magnetic Resonance", McGraw-Hill, New York, 1959.
5. Slichter C.P., Principles of Magnetic Resonance", Harper & Row, New York, 1963.
6. Chan S.I., Kula R.S., Sawyer D.T., Finley C.M., *J. Am. Chem. Soc.*, **35** (1963) 2930.
7. Chan S.I., Kula R.S., Sawyer D.T., *J. Am. Chem. Soc.*, **36** (1963) 377.
8. Miller R.S., Pratt L., *Discussions Faraday Soc.*, **34** (1962) 88.
9. Gutowsky H.S., Holm C.H., *J. Chem. Phys.*, **25** (1956) 1228.
10. Solomon I., *Phys Rev.*, **99** (1959) 559.
11. Bloembergen N., *J. Chem. Phys.*, **27** (1957) 572.
12. Sievers R.A. (ed.), "NMR Shift Reagents", Academic Press, New York, 1973.
13. Nelson W.O., Karpishin T.B., Rettig S.J., Orvig C., *Inorg. Chem.*, **27** (1988) 1045.
14. Clevettte D.J., Nelson W.O., Nordin A., Orvig C., Sjoberg S., *Inorg. Chem.*, **28** (1989) 2079.
15. Finnegan M.M., Rettig S.J., Orvig C., *J. Am. Chem. Soc.*, **108** (1986) 5033.

CHAPTER 4

COMPUTER MODELING

Biological metal ion chelation has now assumed a central role in the study of coordination chemistry. In human blood plasma the metal ions present may be classified into 4 distinct fractions:

i) those which are incorporated rapidly into metalloprotein and are non-exchangeable;

ii) those which are relatively loosely bound by other types of proten and are in labile equlibrium with similar ions in solution;

iii) those which are complexed by the numerous low molecular weight ligands present, including amino-acid anions, carboxylates, carbonates, phosphate, salicylate and ascorbate;

iv) the free metal ions.

It has become generally accepted that the small but significant fraction of metal ions in blood plasma occurring as low molecular weight complexes play an important role in the biological transport of the trace metal ions [1,2]. Indeed, given their small molecular size, such complexes seem to be the only form capable of diffusing through biological membranes into tissue or to be filtered through the kidneys to be excreted in the urine.

It follows that an acquisition of a detailed knowledge of the equilibrium distribution of metal ions between low-molecular-weight ligands is desirable. Simulation of metal ion-equilibria using high speed computers constitutes the only currently available method of estimating the equilibrium concentrations of the complexes involved. Computer simulation of the complex, formation equilibria between the low-molecular-weight ligands and the metal ions of blood plasma has been pioneered by Perrin and his co-workers [3,4]. Perrin's earlier models were restricted to Cu^{2+} and Zn^{2+} together with a selection of amino acids. In later developments the effects of inserting proteins and Ca^{2+} and Mg^{2+} were examined [4]. Because the earlier models are abbreviated examples of the conditions in blood, a need arose for a more comprehensive study. May *et. al* [5,6] have published a computer model of blood and have used this model to explain several observations [7]. The model consists of 40 ligands, 9 metal ions and *ca.* 5000 complexs.

To this model we have added the appropriate constants for Al(III) and Gd(III) in order to investigate the *in vivo* fate of these metal ions. These constants were as far as possible abstracted from the literature [8]. In cases where the same constants had been published by several authors the value of these constants were evaluated critically. Corrections for ionic strength and temperature have been made where possible to produce a set of constants applicable to physiological conditions. In cases where a complex was potentially important, but for which no constants were available, values were estimated. This was done mainly using linear free-energy relationships between Al^{3+}, Gd^{3+} and Fe^{3+}, but in certain cases appropriate interpolations were made based on

chemical analogies. The final set of constants used in this simulation study is given in the Appendix.

Mixed-ligand (ternary) complex formation occurs in systems containing metal-ions and two or more different ligands. These constants have been shown to be important in blood plasma [9]. Since very little data is available on ternary complex formation of Al^{3+} and Gd^{3+} the relevant binary constants were used to calculate the ternary constants [10]. These constants were used in the model to calculate species distribution.

ALUMINIUM

Aluminium readily undergoes extensive hydrolysis in aqueous solution forming an insoluble salt. $Al(OH)_3$. Being amphoteric at higher pH this salt redissolves to form $[Al(OH)_4]^-$. In the presence of phosphate, Al^{3+} can also form the highly insoluable complex $Al(OH)_2(H_2PO_4)$. Aluminium forms very stable binary [11,12] and ternary complexes [13,14]. Because of the high plasma concentration of phosphate it is important that these complexes be included in any model of plasma. The avidity of transferrin for Al^{3+} has been measured under physiological conditions to be 12.9 and 12.3 for $\log K_1$ and $\log K_2$ respectively [15]. At 1 lmol total Al^{3+} per litre of plasma Martin [16] has shown that this leads to a permitted free Al^{3+} concentration of $10^{-14.6}$ mol dm^{-3}. However, if competition with the other components of blood plasma is taken into account a lower free metal concentration is obtained. At

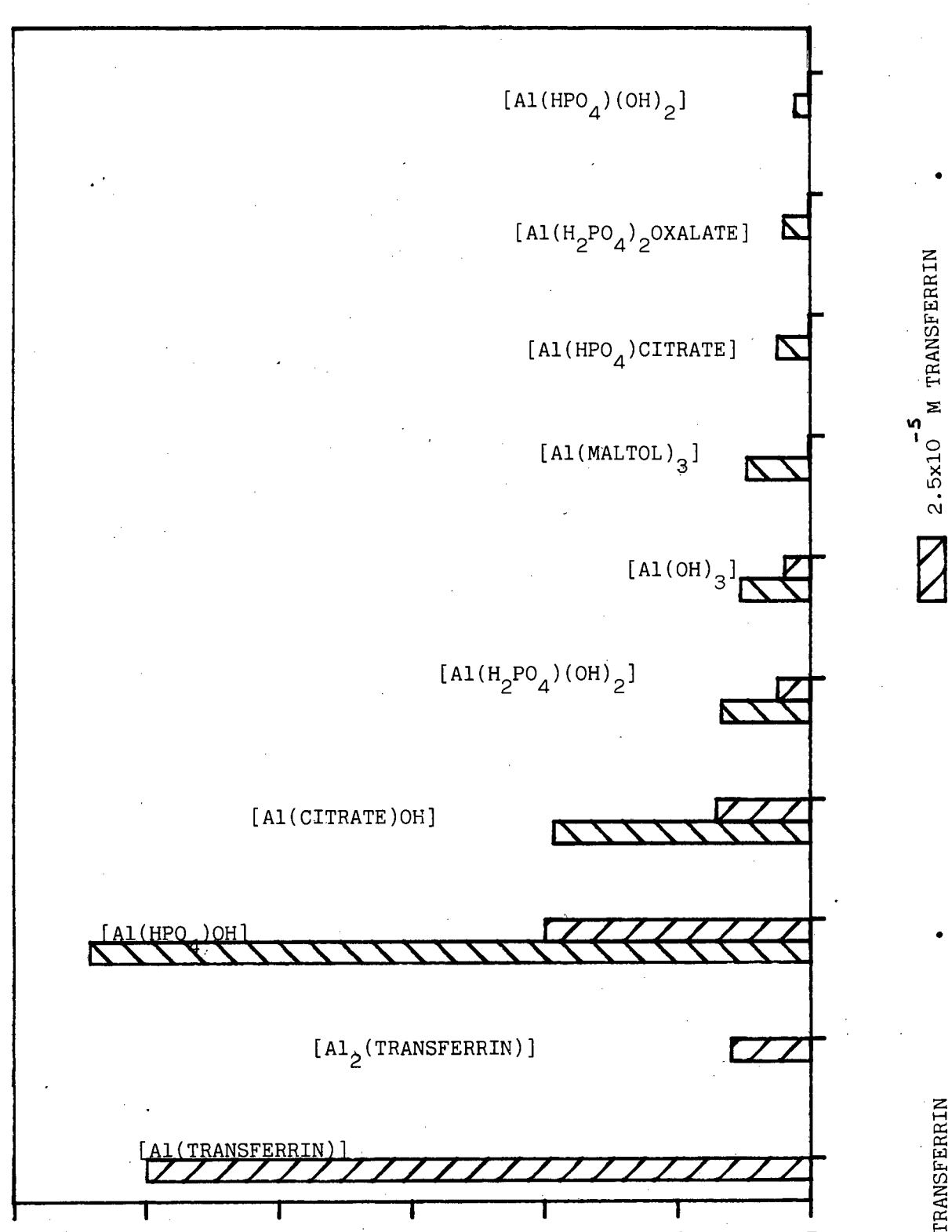

Figure 4.1 Calculated blood plasma species distribution of Al^{3+}.

pH 7.4, within the total aluminium concentration range 10^{-13} - 10^{-15} mol dm^{-3}, *ca.* 50% of the albumin is bound to transferrin in the 1:1 complex [17]. Using this information it is possible to estimate the free Al^{3+} concentration as ~10^{-9} x (Total Al^{3+} concentration). At a total Al^{3+} concentration of 1 lmol this means a free Al^{3+} concentration of 10^{-15} mol dm^{-3}.

Figure 4.1 shows the species distribution of Al^{3+} in blood plasma using the model incorporating the ligand maltol with appropriate, experimentally determined stability constants. Since transferrin uptake is slow, but inevitable, we have considered the species distribution before and after equilibrium with this protein becomes established. This distribution is independent of the Al^{3+} concentration within the range 10^{-13} to 10^{-5} mol dm^{-3}. The effect of the tranferrin is to decrease the amount Al^{3+} available to the low molecular weight pool but the distribution remains the same. The model indicates that only 12% of Al^{3+} exists as the $[Al(maltol)_3)]$ complex (5.3% if transferrin binding is considered). This suggests that the neurotoxicity of the complex may be much greater than implied in the literature [18] since it is only this small fraction of aluminium which exists as the lipophillic, neutral maltol complex which may be capable of crossing the blood-brain barrier.

Maltol was investigated using the Plasma Mobilizing Index, PMI, which is defined as the increase in low molecular weight concentration of a metal-ion brought about by a chelating agent relative to the metal ion concentrations in the absence of the chelating agent. These results

indicate that as the concentration of maltol is increased very little mobilisation of aluminium is observed. At a 10^{-4} mol dm^{-3} maltol concentration log(PMI) for aluminium is 0.05. At this concentration substantial mobilisation of Cu^{2+} and Fe^{3+} is seen. Figure 4.2 shows PMI curves for Al(III) with various other chelating agent.

Since aluminium could disrupt life's essential processes at the cellular level *via* siderophore transport, the kinetics and mechanism of aluminium uptake and release by naturally occurring siderophores is of some significance. This potential toxicity of aluminium has lead to the development of protocols for its removal from the body.

Desferrioxamine (DFO) is currently used as a therapeutic agent in the treatment of transfusion induced iron overload associated with b-thalassemia. The DFO complex with Al^{3+} is of particular interest in that DFO has been employed in chelation therapy to remove aluminium from patients suffering from dialysis encephalopathy, Alzheimer's disease, and other ailments associated with elevated levels of aluminium in the body [19-23]. An experimental stability constant for hexadentate complex formation is available for the Fe^{3+} complex of DFO [24] but not for the Al^{3+} analogue. Schwarzenbach *et al* [24], however, have estimated that the hexadentate Al^{3+} complex would be 7 orders of magnitude less stable than ferrioxamine. This is because dissociation rate constants are larger for Al^{3+} and complexation rate constants are larger for Fe^{3+}. It has been postulated that complexation rates are dominated by water exchange energetics [25] and that the dissociation rates may reflect the greater electronegativity of Fe^{3+} which results in

Plasma Mobilizing Index (*PMI*) of Al^{3+} with several chelating ligands. HBED = N,N'-bis(*o*-hydroxylbenzyl)ethylenediamine-N,N'-diacetic acid; EHPG = ethylene-1,2-bis(*o*-hydroxyphenylglycine); DFO = desferrioxamine; PLED = N,N'-bis(pyridoxyl)ethylenediamine-N,N'-diacetic acid; TIRON = 1,2-dihydroxybenzene-3,5-disulphonate.

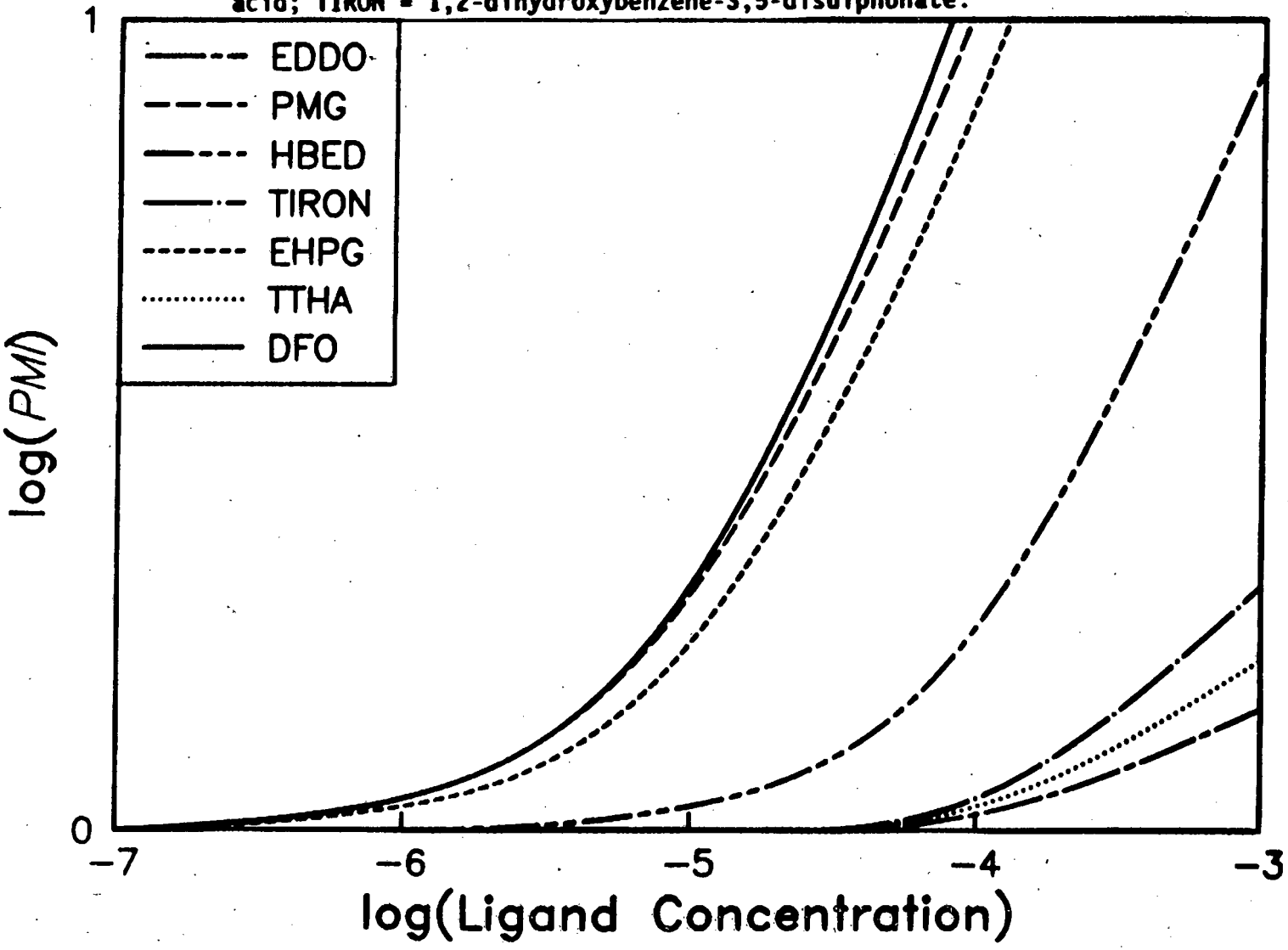

a greater degree of covalent character for the dissociating Fe-O=C bond. Based on kinetic data, Garrison and Crumbliss [25] predict that the difference in overall stability between the fully chelated hexadentate complexes of Fe^{3+} and Al^{3+} with DFO to be significantly less than the seven orders of magnitude previously predicted. This higher than expected stability of the Al^{3+} desferrioxamine system suggests that Al^{3+} concentrations may influence siderophore mediated Fe^{3+} transport through competition.

GADOLINIUM

Figure 4.3 shows the calculated low molecular weight species distribution of Gd(III) in blood plasma at different total metal concentrations. As the total concentration of Gd(III) changes so the species distribution changes. At low concentrations of Gd(III), the metal ion is bound, almost exclusively to citrate, with appreciable amounts of salicylate, glutaminate, threoninate and oxalate complexes starting to form.

As the concentration of gadolinium increases the available amount of citrate and salicylate are exceeded and a new distribution is established. It is interesting to note that the [Gd(citrate)] complex is more predominant than the $[Gd(salicylate)]^+$ complex despite the latter complex being $\sim 10^5$ times more stable than the former. This is due to the difference in pK_a of the two ligands (5.5. and 13.0 respectively) and highlights the fallacy of equilibrium calculations which do not involve competing reactions [26].

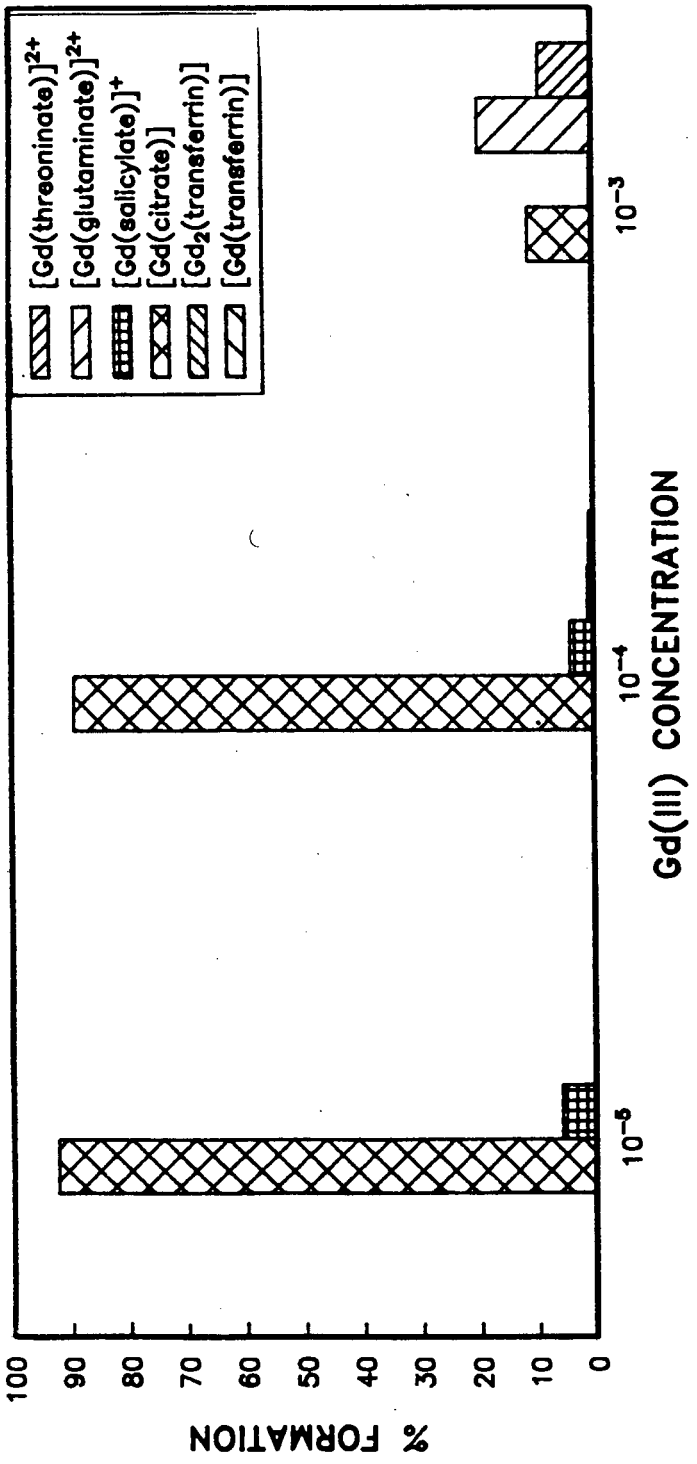

Figure 4.3 Calculated blood plasma species distribution of Gd^{3+}

While it is relatively simple to determine the total Gd(III) concentrations in blood plasma it is more difficult to predict the low molecular concentrations of the metal ion. Since the vivo concentration of transferrin (used to transport iron in the blood) exceeds that of Fe^{3+} it is likely that there will be tranferrin available to coordinate Gd^{3+}. The effect of introducing transferrin into the blood model is shown in Figure 4.4 and indicates that below a concentration of 10^{-4} mol dm^{-3} the Gd(III) is almost exlusively bound to transferrin as the [Gd(transferrin)] and [Gd_2(transferrin)] complexes. At 10^{-3} mol dm^{-3} Gd^{3+}, however, the concentration of available transferrin is exceeded and the transferrin free model is applicable. The affect of transferrin binding on the Gd(III) species distribution is one of lowering the total available Gd(III).

The effect that Gd(III) has on the low molecular weight species distributions of other *in vivo* metal ions is shown in Figure 4.5. The Cu^{2+} species distibution is not significantly affected by the presence of Gd(III). Zn(II), Ca(II) and Fe(III) species distribution are, however, more markedly affected.

Gd(III) displaces Zn(II) from its most predominant cysteinate complexes as it does Ca(II) and Fe(III) from their citrate complexes. These predicted results are in accord with the clinical observations that gadopentetic acid, $[Gd(DTPA)]^{2-}$, can cause slightly elevated iron serum levels and inhibit blood clotting [27,28].

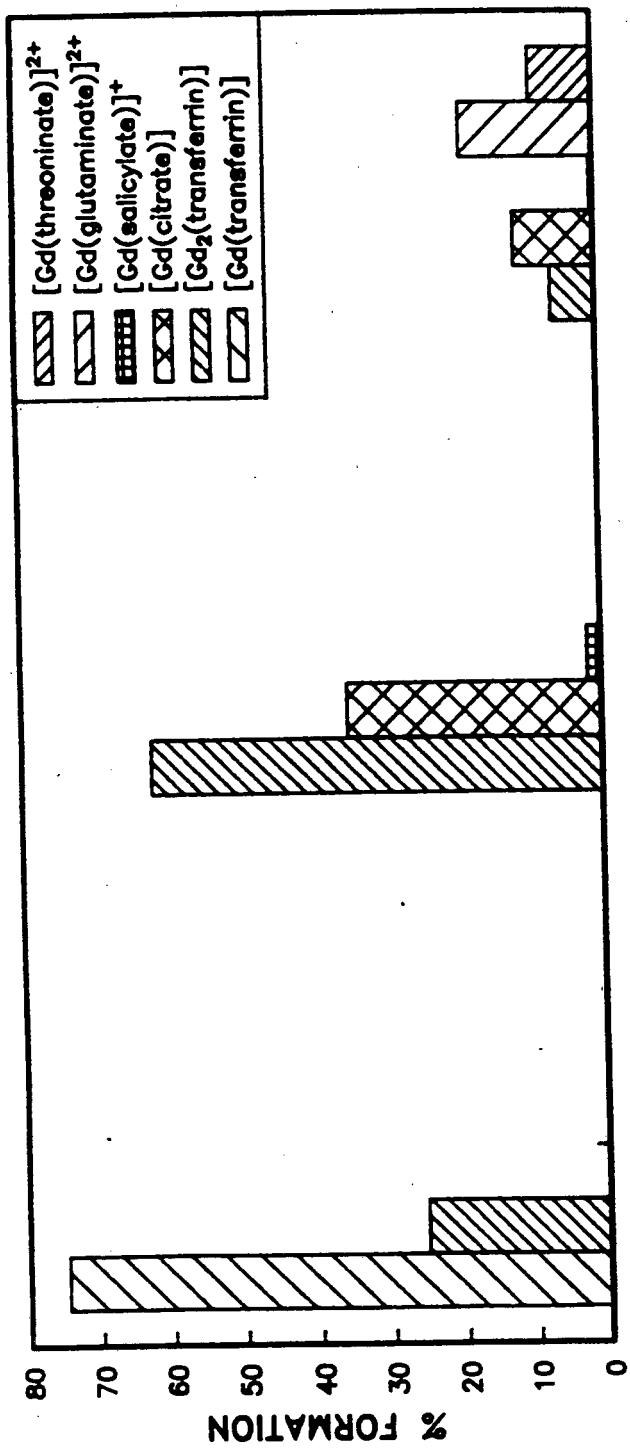

Figure 4.4 The effect of transferrin on Gd^{3+} species distribution

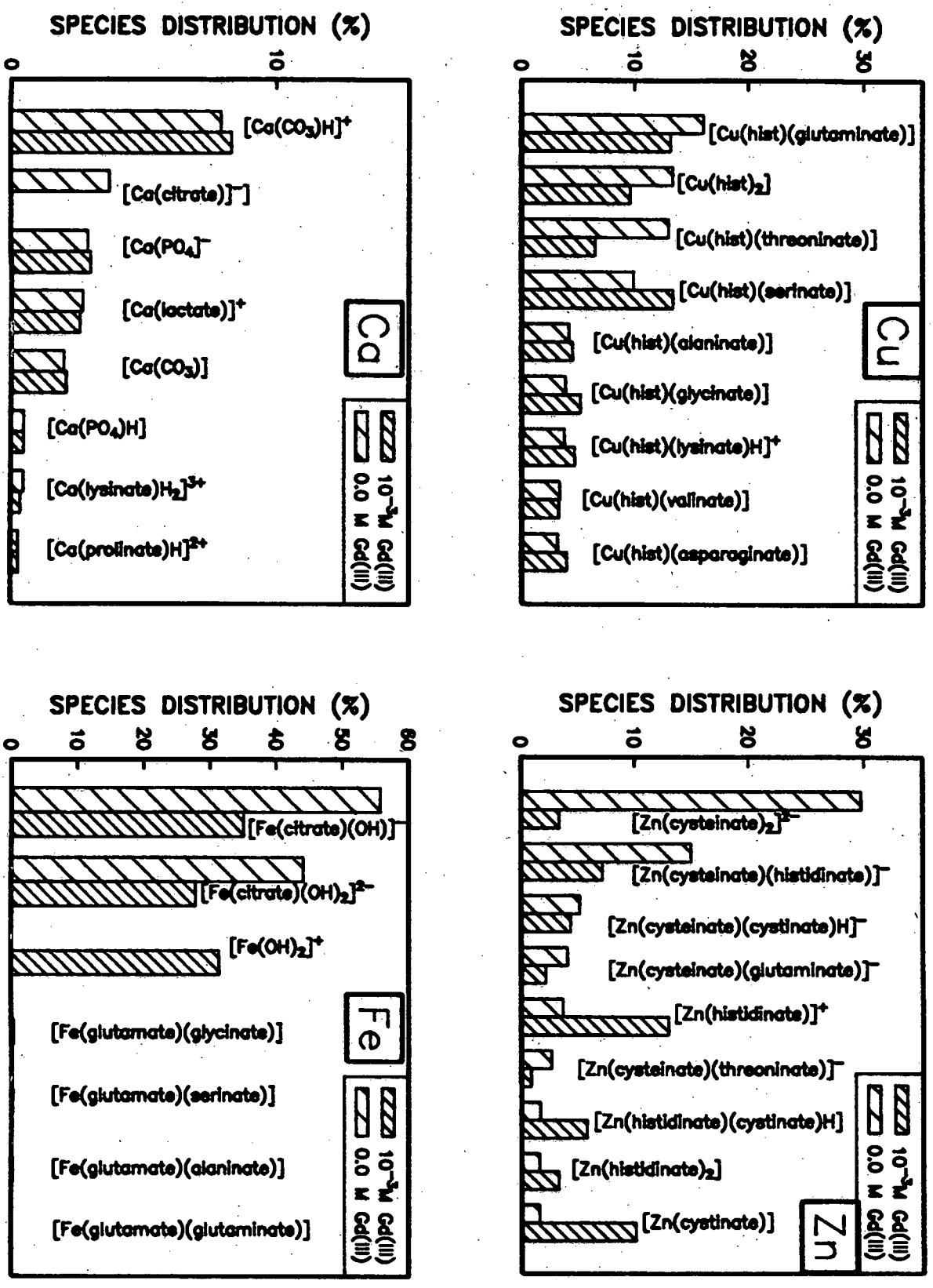

Figure 4.5 Effect of Gd^{3+} on the species distribution of other in vivo metal ions.

Of all elements, gadolinium has the strongest influence on T_1 relaxation times of water protons. Chelating gadolinium to EDTA or DTPA reduces, but far from eliminates, gadolinium's strong influence on proton T_1 and T_2 relaxation. Of interest to the toxicologist and radiologist is the fate of an administered contrast medium. The toxicity of metal complexes can arise either from the toxicity of the intact complex or from the metal-ion or ligand upon complete or partial dissociation of the complex. Whether the chemotoxicity of the Gd-EDTA complex or a dissociation of the gadolinium ion from the EDTA ligand within the body accounts for its low tolerance *in vivo* is not clear. It may be that the stability constant of $\sim 10^{17}$ for Gd-EDTA is insufficient to prevent the interaction of free gadolinium ions with high affinity binding sites of enzymes. DTPA binds gadolinium several times more tightly (logk = 22) than EDTA. Gd^{3+} chelation with DTPA does, in fact, produce a compound with much improved tolerance.

Lauffer has attempted to explain the difference in toxicity in terms of kinetics [29]. Because of its ion size and electronic structure Gd^{3+} forms kinetically very labile complexes which, as in the case of EDTA and DTPA, may also be very stable. The combination of gadolinium with DTPA reduces the toxicity of the two seperate components.

To assess the usefulness of gadolinium-maltol complex as an NMR contrast agent, the appropriate formation constants were added to the computer model of blood plasma. The species distributions of Gd^{3+} in blood plasma in the presence of maltol is given in Table 4.1. These results

Table 4.1 Calculated blood plasma species distribution of Gd^{3+}.

Species	Concentration	%Total Gd^{3+}
[Gd(citrate)]	1.7×10^{-6}	88.2
$[Gd(salicylate)]^{+}$	1.2×10^{-7}	6.1
$[Gd(maltol)(lactate)]^{+}$	2.3×10^{-8}	1.2
$[Gd(maltol)_2]^{+}$	1.8×10^{-8}	0.9
$[Gd(maltol)]^{2+}$	1.5×10^{-8}	0.8
[Gd(maltol)(cysteinate)]	1.1×10^{-8}	0.6
$[Gd(maltol)(histidinate)]^{+}$	5.2×10^{-9}	0.3
$[Gd(glycinate)]^{2+}$	4.8×10^{-9}	0.2
[Gd(maltol)(malate)]	4.2×10^{-9}	0.2
$[Gd(threoninate)]^{2+}$	3.6×10^{-9}	0.2
[Gd(maltol)(sulphate)]	2.7×10^{-9}	0.1

Figure 4.6 Plot of T_1 against the logarithm of the ligand concentration. MAL = maltol; DTPA = diethylenetriaminepentaacetate; DMDO = N,N'-di-(2-dimethyl)ethyloxamide; TTDA = 3,6,9,12-tetra-azatetradecanedioate.

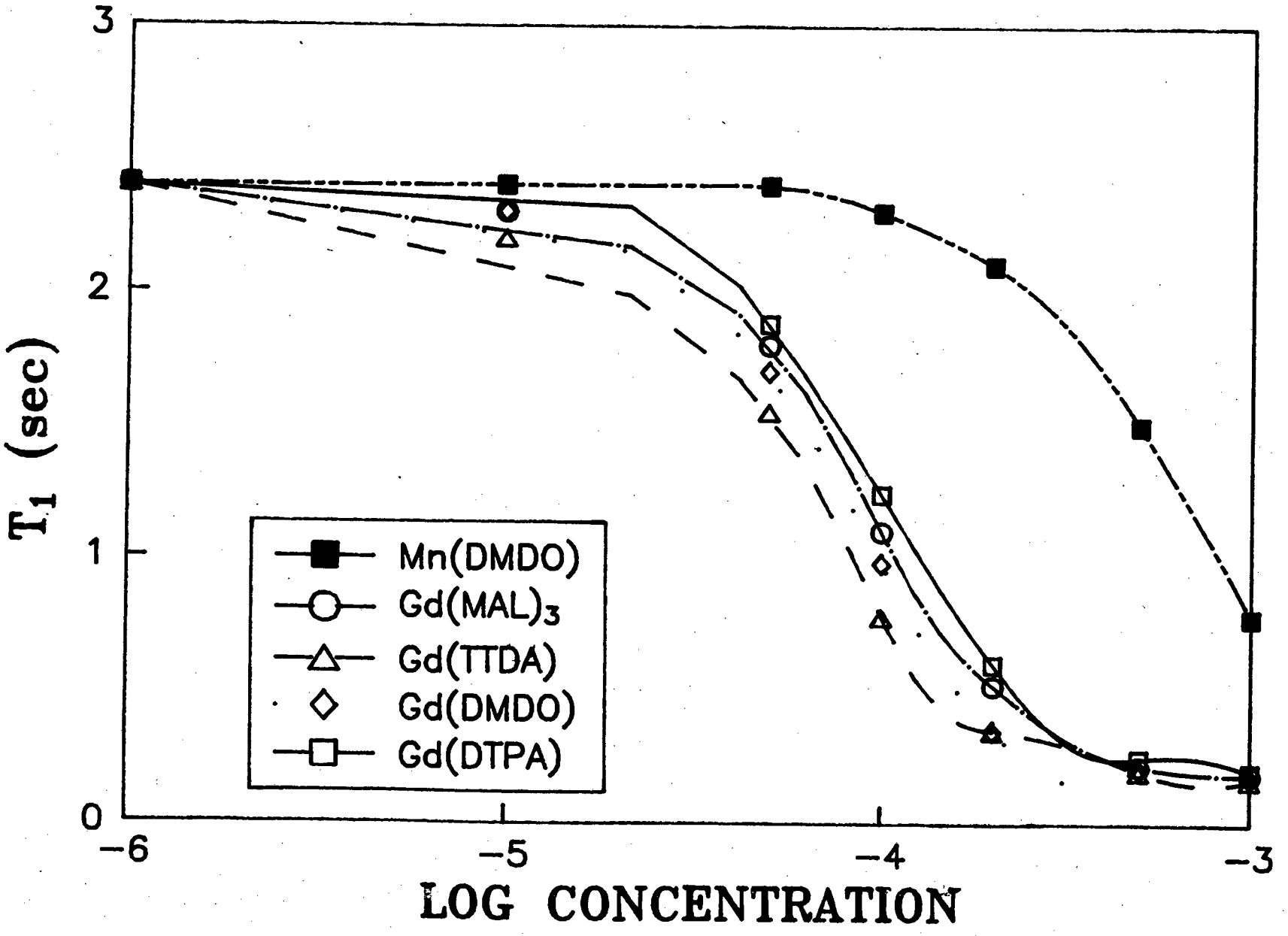

suggest that the Gd-maltol complex is unlikely to survive *in vivo* since no $[Gd(maltol)_3]$ is observed even at a metal concentration of 10^{-3} M.

Prior to the above results it was hoped that the $[Gd(maltol)_3]$ complex would be a useful constrast agent, which, by analogy with $[Al(maltol)_3]$, would cross the blood brain barrier. For this reason the relaxivity of Gd-maltol was measured. The results, presented in Figure 4.6, show the relaxivity of Gd-maltol to be similar to that of Gd-DTPA, a reagent which has been used successfully as a contrast agent [30]. This highlights the fact that the relaxation enhancement brought about by metal complexes in biological fluids depends on the distribution/fate of the complex *in vivo*. The $[Gd(DTPA)]^{2-}$ complex is stable *in vivo* (within the time limit of the diagnostic procedure) and so is a useful MRI contrast agent. $[Gd(maltol)_3]$, which has the same relaxivity as $[Gd(DTPA)]^{2-}$ is not stable *in vivo* and so is not useful as an MRI contrast agent. In fact we would predict that $[Gd(maltol)_3]$ would be toxic.

INDIUM

The most obvious requirement an indium complex must meet if it is to be a useful radiopharmaceutical is the ability to resist hydrolysis at physiological pH. Other properties that an indium complex should possess, if it is to be capable of crossing the blood brain barrier include lipophilicity, electroneutrality and relative low molecular weight.

on multidentate ligands where the chelate effect produces a synergistically enhanced binding stability.

Like Al^{3+}, In^{3+} undergoes extensive hydrolysis in aqueous solution, forming the insoluble $In(OH)_3$ salt. It is for this reason that the radionuclide ^{111}In is supplied with a high background concentration of acid or citrate.

Since the appropriate formation constants for indium were not available for inclusion in our computer model of blood, we have considered the *in vivo* fate of gallium. Both gallium and indium are members of Group IIIA of the Periodic Table and may be expected to resemble each other chemically.

Our computer simulation of blood plasma has shown that at metal-ion concentrations likely to be encountered in nuclear imaging ($\sim 10^{-9}$ M), the Ga^{3+} is bound almost exclusively to transferrin. It has been shown [31] that under identical conditions gallium binds to transferrin to a lesser degree than does indium. Increasing the amount of Ga^{3+} so that the transferrin binding sites are saturated means that the solubility of $Ga(OH)_3$ and $Ga(PO_4)$ is exceeded and the formation of colloidal gallium is expected. Indium, also being hydrolytically unstable, is expected to behave similarly.

Kinetic inertness towards the ubiquitous iron transport protein requires the complexation of the metal ions, In^{3+} and Ga^{3+}, by a multidentate chelating ligand. This probably accounts for the chemical focus being on multidentate ligands where the chelate effect produces a synergistically enhanced binding stability.

In view of the preceeding discussion we conclude that the complexes resulting from coordination of In^{3+} by maltol or analogs of maltol, are unlikely to be stable enough *in vivo* to prevent exchange of In^{3+} with transferrin and will thus not be useful in the field of diagnostic medicine.

In this study we have used a plasma model as an aid to understanding the *in vito* fate and possible toxicity of the maltol complexes of Al^{3+}, In^{3+} and Gd^{3+}. It must, however, be emphasized that any computer model is only as good as the data upon which it is based and that many of the constants used in our model have been estimated or determined under inappropriate conditions. In spite of these limitations the model has been successful in explaining many clinically observed phenomena.

REFERENCES

1. Williams D.R., "The Metals of Life", Van Nostrand Reinhold, London, 1971.
2. Saltman P., *J. Chem Ed.*, **42** (1965) 682.
3. Perrin D., *Nature*, **206** (1965) 170.
4. Perrin D., Hallman P.S., *Biochemistry*, **121** (1971) 549.
5. May P.M., Williams D.R., Linder P.W., *J.Chem Soc. Dalton*, 588 (1977).
6. Berthon G., Hacht B., Blais M., May MP.M., *Inorg. Chim. Acta*, 125 (1986) 219.
7. May P.M., Williams D.R. *FEBS Lett.*, **78** (1977) 134.
8. Martell A.E., Smith R.M., Critical Stability Constants", Vols 1-4, Plenum Press, New York, (197478).
9. Sigel H., "Advances in Solution Chemistry", Bertin I., Lunazzi L., Dei A. (eds.), Plenum Press, New York, 1981.
10. Marcus Y., Eliezer I., *Coord. Chem. Rev.*, **44** (1969) 273.
11. Jackson G.E., Voyi K., *S. Afr. J. Chem.*, **41** (1988) 17.
12. Jackson G.E., Voyi K., *Polyhedron*, **6** (1987) 2095.
13. Ramamoorthy S., Manning P., *J. Inorg. Nucl. Chem.*, **37** (1975) 363.
14. Arp P., Meyer W., *Can. J. Chem.*, **63** (1985) 3357.
15. Martin R., Savory Y., Brown S., Bertholf R., Wills M., *Clin. Chem.*, **33** (1987) 405.
16. Martin R., *Clin. Chem.*, **32** (1986) 1797.
17. Jackson G.E., *Polyhedron*, in press.
18. Finnegan M.M., Rettig S.J., Orvig C.J., *J. Am* Chem. Soc., 108 (1986) 5033.

19. Griswold W., Reznik V., Mendova S., Trauner D., Alfrey A., *Pediatrics*, 71 (1983) 56.

20. Andreoli S., Bergstein J., Sherrard D., *N. Engl. J. Med.*, 310 (1984) 1079.

21. Wurtman R., *Sci Am.*, **252** (1985) 62.

22. Perl D., Brody A., *Science* , **208** (1980) 297.

23. Meyer J., Thomas W., *Kidney Int.*, **29** (1986) 520.

24. Anderegg G., L'Eplattenier F., Schwarzenbach G., *Helv. Chim. Acta*, **46** (1963) 1409.

25. Garrison J.M., Crumbliss A.L., *Inorg. Chim. Acta*, **138** (1987) 61.

26. Jackson G.E., Wynchank S., Woudenberg M., *Mag. Res. Med.*, in press.

27. Sax I.N., "Dangerous Properties of Industrial Materials", 5 th. ed., Van Nostrand Reinhold, New York, 1984.

28. Chasteen N.D., Thompson C.P., Martin D.M., "The release of iron from transferrin. An overview", in Frontiers in Bioinorganic Chemistry, A. Xavier (ed.), VCH, Weinheim, 1986.

29. Lauffer R.B., *Chem. Rev.*, **87** (1987) 902.

30. Carr D.H., Brown J., Bydder G.M., *et. al*, *Lancet*, 1 (1984) 484.

31. Moerlein S.M., Welch M.S., *Int. J. Nucl. Med.*, **8** (1981) 277.

A P P E N D I X

Table A.1. Binary Al^{3+} and Ga^{3+} stability constants used in blood model.

L	*p*	*q*	*r*	logβ	ref	L	*p*	*q*	*r*	logβ	ref
						Al^{3+}					
tartrate	1	1	-1	1.18	1	carbonate	2	1	-4	-20.4	5
	1	2	0	7.65	1		3	1	-5	-22.7	5
	1	1	-2	-3.97	1	hydroxide	1	0	-1	-5.10	6,
	1	2	-1	3.93	1		1	0	-2	-10.4	7,
	1	2	-3	-8.74	1		1	0	-3	-15.9	5
	1	3	-4	-26.8	1		1	0	-4	-24.1	
	1	3	-6	-39.5	1		3	0	-11	-54.8	
transferrin	1	1	0	12.9	2		6	0	-15	-49.5	
	2	1	0	25.2	2		8	0	-22	-76.5	
salicylate	1	1	0	12.7	3	fluoride	1	1	0	7.01	8
	1	2	0	23.11	3		1	2	0	12.75	8
	1	2	-1	15.51	3		1	3	0	17.02	8
	1	2	-2	6.19	3		1	4	0	19.72	8
oxalate	1	1	0	5.02	4		1	5	0	20.91	8
	1	2	0	9.33	4	phosphate	1	1	0	11.4	9,
	1	3	0	12.41	4		1	1	1	20.5	10
	1	1	-1	-0.51	4		1	1	2	25.8	
	1	1	-2	-8.59	4	cysteinate	1	2	0	6.43	10
malonate	1	1	0	6.3	4	succinate	1	1	-1	-0.25	4
	1	2	0	11.1	4		2	1	-1	2.88	4
	1	3	0	13.3	4		1	1	-2	-5.19	4
	1	1	-1	0.79	4	HBED	1	1	0	29.4	b
	1	2	-2	-7.42	4	EHPG	1	1	0	25.2	b

Table 1 cont.

citrate[a]	1	1	0	8.0	11,	EDDO	1	1	0	16.6	b
	1	1	-1	4.6	12,		1	1	1	20.6	b
	1	1	1	10.2	13		1	1	2	22.6	b
	1	2	0	13.0			1	1	-1	9.7	b
						Ga^{3+}					
phosphate	1	1	1	18.8	8	oxalate	1	1	0	6.45	8
	1	1	0	10.0	b		1	2	0	12.38	8
	1	1	2	19.5	8		1	3	0	17.86	8
citrate[a]	1	1	1	11.6	14,		1	1	-1	2.0	b
	1	1	-1	7.1	15		1	1	-2	-4.0	b
	1	1	0	10.02		malonate	1	1	0	2.4	b
	1	2	0	15.3	b		1	2	0	3.6	b
hydroxide	1	0	-1	-3.31	6,	transferrin	1	1	0	20.3	17,
	1	0	-2	-6.76	16		2	1	0	39.6	b
	1	0	-3	-11.16	16	salicylate	1	1	0	16.1	14
	1	0	-4	-17.17	16	tartrate	1	1	0	18.5	14

a neutral ligand H_3citrate.

b Estimated.

1. M. Walser, *J. Clin. Invest.*, 1961, 40, 723.

2. R. Martin, Y. Savory, S. Brown, R. Bertholf and M. Wills, *Clin. Chem.*, 1987, 33, 405.

3. L. Ohman and S. Sjoberg, *Acta Chem. Scand.*, 1983, **A37**, 875.

4. G. Jackson and A. Cosgrove, *S. Afr. J. Chem.*, 1982, 35, 93.

5. L. Ohman and W. Forsling, *Acta Chem. Scand.*, 1981, **A35**, 795.

6. C. Baes and R. Mesmer, "The Hydrolysis of Cations", John Wiley & Sons, New York, 1976.

7. G. Berthon and M. Venturini, *J. Chem. Soc. Dalton*, 1987, 1145.

8. A.E. Martell and R.M. Smith, "Critical Stability Constants," Vols. 1-4, Plenum Press, New York, 1974-79.

9. G.E. Jackson and K. Voyi, *S.Afr. J. Chem.*, 1988, **41**, 17.

10. S. Ramamoorthy and P. Manning, *J. Inorg. Nucl. Chem.*, 1975, **37**, 363.

11. R. Martin, *J. Inorg. Biochem.*, 1986, **28**, 181.

12. L. Ohman, *Inorg. Chem.*, 1988, **27**, 2565.

13. G. Jackson, *S. Afr. J. Chem.*, 1982, **35**, 89.

14. N. Skorik and A. Artish, *Russ. J. Inorg. Chem.*, 1985, **38**, 1130.

15. W. Harris and A. Martell, *Inorg. Chem.*, 1976, **15**, 713.

16. P. Brown, *J. Chem. Soc. Dalton*, 1989, 399.

17. S. Moerlein and M. Welch, *Int. J. Nucl. Med. Biol.*, 1981, 8, 277.

Table A.2. Important ternary Al^{3+} and Ga^{3+} stability constants used to construct blood model. Other ternary constants calculated automatically using MIX.

Species	logβ	Reference
$[Al(citrate)(malonate)]^{2-}$	12.05	a
$[Al(citrate)(salicylate)]^{2-}$	20.0	a
$[Al(citrate)(oxalate)]^{2-}$	11.2	a
$[Al(citrate)(cysteinate)]^{2-}$	14.9	1
$[Al(HPO_4)(malonate)]^{-}$	25.3	1
$[Al(H_2PO_4)(malonate)]$	30.6	1
$[Al(HPO_4)(salicylate)]^{-}$	29.56	2
$[Al(H_2PO_4)(salicylate)]$	34.16	2
$[Al(HPO_4)(oxalate)]^{-}$	24.8	a
$[Al(H_2PO_4)(oxalate)]$	28.3	2
$[Al(HPO_4)_2(oxalate)]^{3-}$	42.1	2
$[Al(HPO_4)(cysteinate)]^{-}$	15.66	a
$[Al(HPO_4)(citrate)]^{2-}$	26.5	2
$[Al(H_2PO_4)(citrate)]^{-}$	30.38	2
$[Al(HPO_4)(OH)]$	28.6	a
$[Al(HPO_4)(OH)_2]^{-}$	32.8	a
$[Al(H_2PO_4)(OH)]^{+}$	33.5	a
$[Al(H_2PO_4)(OH)_2]$	41.0	a
$[Al(H_2PO_4)(OH)_3]^{-}$	45.8	a

cont.

Table A.2 cont.

Species	logβ	Reference
$[Ga(HPO_4)(OH)]$	27.3	a
$[Ga(HPO_4)(OH)_2]^-$	35.0	a
$[Ga(H_2PO_4)(OH)]^+$	28.5	a
$[Ga(H_2PO_4)(OH)_2]$	37.4	a
$[Ga(H_2PO_4)(OH)_3]^-$	44.7	a
$[Ga(HPO_4)(oxalate)]^-$	24.7	a
$[Ga(H_2PO_4)(oxalate)]$	25.4	a
$[Ga(HPO_4)(citrate)]^{2-}$	26.5	a
$[Ga(H_2PO_4)(citrate)]^-$	30.38	a

a Estimated.

1. S. Ramamoorthy and P. Manning, *J. Inorg. Nucl. Chem.*, 1975, 37, 363.

2. P. Arp and W. Meyer, *Can. J. Chem.*, 1985, **63**, 3357.

Table A.3. Gadolinium(III) formation constants used in this study.
M = Gd(III), L = Ligand.

Formula	Ligand	Log stability constant	Reference
ML	aminobutanoate	5.6	a
ML	alaninate	5.6	5
ML	argininate	5.4	a
ML	asparaginate	4.3	5,2
ML	aspartate	5.74	3
ML_2		10.5	
ML	citrullinate	5.4	a
ML	cysteinate	7.825	4
ML_2		14.90	
ML	glutaminate	5.3	a,5
ML	glutamate	5.6	6
ML	glycinate	3.26	7
MLOH		-4.96	
ML	histidinate	4.9	8
MLH		11.3	
ML_2		9.16	
ML	hydroxyprolinate	5.08	9
ML	isoleucinate	5.6	a
ML	leucinate	5.6	a
ML	lysinate	7.0	10
ML_2		13.4	
ML	methioninate	5.6	a

Table A.3. continued\

Formula	Ligand	Log stability constant	Reference
ML	ornithinate	5.6	a
ML	phenylalaninate	3.6	8
ML	prolinate	5.6	9,11
ML	threoninate	5.6	a
ML	tryptophanate	5.2	8
ML_2		9.8	
ML	tyrosinate	4.92	8
ML_2		9.35	
ML	valinate	5.65	a
M_2L_3	carbonate	-32.2	3
ML	phosphate	-22.26	3
ML	sulphate	3.0	3
ML_2		5.0	
ML	thiocyanate	0.21	3
ML	ammonia	0.7	7
ML	citrate	7.83	3
ML	lactate	2.83	3,12
ML_2		5.0	
ML_3		6.10	
ML	malate	4.76	3
ML_2		7.0	
ML	oxalate	5.4	3

Table A.3. continued\

Formula	Ligand	Log stability constant	Reference
ML	pyruvate	1.97	a
ML_2		3.32	
ML_3		3.79	
ML	salicylate	13.0	3
MLH		15.0	
MLH	succinate	7.02	3
ML_2H_2		17.4	
ML	histaminate	0.9	a
ML	transferrin	13.0	a
M_2L		25.7	

a estimated - see text.

1. N.D. Chasteen, C.P.Thompson and D.M. Martin, *The Release of Iron from Transferrin. An Overview*, in Frontiers in Bioinorganic Chemistry, A. Xavier (ed), VCH, Weinheim, (1986).

2. S.D. Makhijani and S.P. Sangal, *J. Indian Chem. Soc.*, 54, 670 (1977).

3. A.E. Martell and R.M. Smith, *Critical Stability Constants*, Vols. 1-4, Plenum Press, New York (1974-79).

4. C.L. Sharma and T.K. De, *J. Less-Common Met.*, 70, 63 (1980).

5. F. Khan, *J. Indian Chem. Soc.*, **63**, 340 (1986).

6. R.C. Agarwal and S.L. Agarwal, *Thermochim. Acta*, **44**, 121 (1981).

7. R.D. Hancock, G.E. Jackson and A. Evers, *J. Chem. Soc., Dalton Trans.*, 1384 (1979).

8. L.D. Pettit, *Pure Appl. Chem.*, **56**, 247 (1984).

9. S. Zielinski, L. Lomozik and A. Wojciechowska, *Monatshefte fur Chemie*, **112**, 1245 (1981).

10. R.S. Saxena and S.K. Dhawan, *Indian J. Chem.*, **22A**, 89 (1983).

11. R.S. Saxena and A. Gupta, *Indian J. Chem.*, **23A**, 785 (1984).

12. N.K. Mohanty, *Indian J. Chem.*, **22A**, 820 (1983).